

BIOKINETIC BEHAVIOUR OF *Chlorella vulgaris*
IN A CONTINUOUSLY STIRRED BIOREACTOR AND
A CIRCULATING LOOP PHOTOBIOREACTOR

A Thesis Submitted to the College of
Graduate Studies and Research
in Partial Fulfillment of the Requirements
for the Degree of Master of Science
in the Department of Chemical Engineering
University of Saskatchewan
Saskatoon

By
DIVYA SASI

PERMISSION TO USE

In presenting this thesis in partial fulfillment of the requirements for a Postgraduate degree from the University of Saskatchewan, I agree that the Libraries of this University may make it freely available for inspection. I further agree that permission for copying of this thesis in any manner, in whole or in part, for scholarly purposes may be granted by the professor or professors who supervised my thesis work or, in their absence, by the Head of the Department or the Dean of the College in which my thesis work was done. It is understood that any copying or publication or use of this thesis or parts thereof for financial gain shall not be allowed without my written permission. It is also understood that due recognition shall be given to me and to the University of Saskatchewan in any scholarly use which may be made of any material in my thesis.

Requests for permission to copy or to make other uses of materials in this thesis/dissertation in whole or part should be addressed to:

Head of the Department of Chemical Engineering

University of Saskatchewan

Saskatoon, Saskatchewan S7N 5C5

Canada

OR

Dean

College of Graduate Studies and Research

University of Saskatchewan

107 Administration Place

Saskatoon, Saskatchewan S7N 5A2

Canada

Biokinetic Behaviour of *Chlorella vulgaris* in a Continuously Stirred Bioreactor and a Circulating Loop Photobioreactor

ABSTRACT

Capture of CO₂ by algae is an important mechanism for removal of this greenhouse gas from the atmosphere. For this reason, *Chlorella vulgaris* has been studied extensively over the years. A high growth rate of the microalgae is essential in order to increase the fixation rate of CO₂ through photosynthesis. Though a number of studies have been carried out to optimize growth of *C. vulgaris*, high growth rates have not been achieved (Kleinheinz & Keffer, 2002).

In this study, a novel circulating loop photobioreactor with enhanced light distribution, gas mass transfer rate and mixing properties was used for the biokinetic study of *C. vulgaris*. The objective was to study individual effects of light intensity and CO₂ concentration on the specific growth rate of *C. vulgaris*. Studies in this photobioreactor could generate high growth rates of 0.043 h⁻¹. The effect of light intensity on the growth of the *C. vulgaris* was determined by varying intensity of light to the photobioreactor within a range of 26.945 mW to 431.128 mW, while the flow of air and CO₂ were held constant. An increase in light intensity to the photobioreactor resulted in an increase in cell density and variation in the chlorophyll content of the *C. vulgaris* cells. Enhanced growth rates of *C. vulgaris* cells in this novel circulating loop photobioreactor could be attributed to the combined effect of the CO₂ concentration and the uniform distribution of light throughout the reactor volume.

Interacting effects of dilution rate, light intensity and concentration of carbon dioxide on specific growth rate was studied in an externally illuminated, continuous flow stirred bioreactor. Steady flow of nutrient medium and air flow was maintained in the bioreactor. This study proved that the dilution rate has major significance at high concentrations of CO₂ and high intensities of light. At high concentrations of CO₂ at 10% (v/v) and 15% (v/v), increasing dilution rate from 0.005 h⁻¹ to 0.01 h⁻¹ could result in increasing growth rate by a factor of 1.45 and 2.16 respectively.

ACKNOWLEDGEMENTS

I wish to offer my heartfelt gratitude to Dr. Gordon Hill for his constant guidance and support during the course of my Masters degree. His supervision was vital. I would like to thank the members of my committee, Dr. Richard Evitts, Dr. Soltan Mohammedzadeh and my external examiner Dr. Charles Maule for their valuable advice.

I would also like to thank the entire faculty and staff in the department of Chemical Engineering. Mr. Henry Berg and Mr. Kevin Jeffery in the Engineering Shops deserve special mention for their prompt service and amazing skill in building the bioreactor.

I appreciate all the support that Ms. Andrea Vigueras has provided for me in the laboratory for the last two months of my research. I also thank Ms. Erin Powell for her constant assistance and invaluable friendship. I am also indebted to all my other friends at the University who have made these past two years memorable.

Lastly, I would like to thank my family for their love and constant support, without which this would not have been possible.

TABLE OF CONTENTS

Permission to Use	i
Abstract	ii
Acknowledgements	iv
Table of Contents	v
List of Tables	viii
List of Figures	ix
List of Abbreviations	xi
Nomenclature	xii

1.0 Introduction

1.1	Motivation for biocapture of Carbon dioxide	1
1.2	Literature review	3
1.2.1	Microbial growth kinetics	3
	Microbial growth phases	3
1.2.2	Growth of <i>Chlorella vulgaris</i>	5
1.2.3	Algae and photosynthesis	7
	Light dependant reactions	7
	Light independent reactions	7
	Significance of light - dark cycle	8
1.2.4	Algae and photobioreactors	8
	Use of circulating loop photobioreactor in fed batch mode	8
	Use of a continuous flow photobioreactor	9
1.2.5	Microbial fuel cells	9
	Metabolism of microbiological cells used in MFC	10
	Classification of MFC's	10
	Microbial anodic half cells	11
	Microbial cathodic half cells	12

Complete microbial fuel cells	14
1.2.6 Use of algae in microbial fuel cells	15
1.3 Knowledge gap and scope for work	16
1.4 Description of following chapters	17
 2.0 Effect of Light Intensity and CO₂ on Growth of <i>Chlorella vulgaris</i> In a Novel Circulating Loop Photobioreactor	
2.1 Introduction	18
2.2 Experimental setup and procedures	19
2.2.1 Photobioreactor	19
Specifications of photobioreactor	19
Material of construction	21
Illumination of the photobioreactor	21
Mixing of reactor volume	23
Circulation	23
2.2.2 Experimental studies	24
Yield of biomass	24
Effect of light intensity	25
Effect of light and dark phases	25
Effect of CO ₂ concentration	25
Yield of chlorophyll	27
Yield of lipids	28
2.3 Results and discussions	29
2.2.3 Yield of biomass	29
2.2.4 Effect of light intensity on growth rate of <i>C. vulgaris</i>	32
2.2.5 Effect of light – dark cycle on growth rate of <i>C. vulgaris</i>	33
2.2.6 Effect of CO ₂ concentration on growth rate of <i>C. vulgaris</i>	34
2.2.7 Yield of chlorophyll and lipids	36
2.4 Reproducibility	38

3.0 Effect of Light Intensity and CO₂ on Growth of *Chlorella vulgaris* In a Continuous Flow Mixed Photobioreactor

3.1	Introduction	39
3.2	Experimental setup and procedures	39
2.2.8	Cells and media	39
2.2.9	Experimental setup	40
2.2.10	Analytical methods used	44
	Measurement of biomass	44
	Determination of cell density using Petrov-Hauser counter	45
3.3	Results and discussions	47
2.2.11	Yield of biomass	47
2.2.12	Effect of dilution rate, concentration of CO ₂ and light intensity on growth rate	50
3.4	Reproducibility	53

4.0 Conclusions and Recommendations

4.1	Conclusions	54
4.1.1	Novel circulating loop photobioreactor	54
4.1.2	Continuous flow mixed photobioreactor	55
4.2	Recommendations	57
4.2.1	Novel circulating loop photobioreactor	57
4.2.2	Continuous flow mixed photobioreactor	58

5.0 References

6.0 Appendices

A - Calculation of Light Intensity Incident on Continuous Flow Mixed Photobioreactor	66
B - Calculation of Circulation Velocity in Circulating Loop Photobioreactor	69
C - Calculation of Biolipid concentration of <i>C. vulgaris</i> by Soxhlet Extraction Method	71

LIST of TABLES

Table 2.1	Specifications of the circulating loop photobioreactor	19
Table 2.2	Specifications of LED lights used for the circulating loop photobioreactor	22
Table 2.3	Yield of biomass obtained at condition (i) with no additional dark phase	31
Table 2.4	Yield of biomass obtained at condition (ii) with 8 hour dark phase	31
Table 2.5	Effect of various parameters on the growth rates of <i>Chlorella vulgaris</i> at 10% (v/v) of CO ₂	32
Table 2.6	Effect of continuous 8 hour dark phase on the specific growth rate of <i>C. vulgaris</i>	34
Table 2.7	Effect of CO ₂ concentration on the specific growth rate of <i>C. vulgaris</i>	35
Table 2.8	Lipid concentration of <i>C. vulgaris</i>	37
Table 2.9	Reproducibility of growth rate data from the circulating loop photobioreactor	38
Table 3.1	Effect of various parameters on the growth rates of <i>Chlorella vulgaris</i>	52
Table 3.2	Reproducibility of growth rate data obtained from the continuously stirred photobioreactor	53
Table A.1	Readings obtained from spectrophotometer when light source was placed at 10 centimeters from surface of bioreactor and when no light source was used.	66
Table B.1	Data table showing calculated values of average circulation velocity for the circulating loop photobioreactor at varying heights of liquid in the reactor.	69

LIST of FIGURES

Figure 1.1	Typical growth curve for batch cell cultivation. The growth of the microbe follows the various phases; lag phase (A), exponential growth phase (B), stationary phase (C) and death phase (D). (Bailey and Ollis, 1986)	5
Figure 1.2	(A) A typical microbiological fuel cell with the essential components; anode, cathode, a proton exchange membrane and an external circuit connecting the two electrodes. (B) Schematic showing the processes occurring at the anode. Electrons produced due to the metabolic reactions in the cell are captured by mediator molecules to the anode, which then moves along the external circuit to produce current. (Powell et al., 2009b)	12
Figure 1.3	(A) A typical microbiological fuel cell with the essential components; anode, cathode, a proton exchange membrane and an external circuit connecting the two electrodes. (B) Schematic showing the processes occurring at the cathode. Electrons from the anode are used to run the metabolic reactions of the microbes at the cathode. (Powell, et al., 2009b)	13
Figure 2.1	Novel circulating loop photobioreactor containing the photosynthetic algae <i>C. vulgaris</i> operating in fed-batch mode.	20
Figure 2.2.	Schematic of LED Strip.	21
Figure 2.3	Scan of light irradiance from the LED bulb.	22
Figure 2.4	Light and dark phases maintained in the circulating loop photobioreactor illuminated with LED lights.	23
Figure 2.5	Variation in average circulation velocity in the circulating loop photobioreactor with change in height of liquid in the reactor.	24

Figure 2.6	Glass bulb used to measure biomass yield of <i>C. vulgaris</i>	26
Figure 2.7	Experimental set-up used to study the pattern of CO ₂ evolution from the circulating loop photobioreactor containing the photosynthetic algae <i>C. vulgaris</i> .	26
Figure 2.8	Transient changes in dry cell weight of <i>C. vulgaris</i> at radiant flux of 26.945 mW.	29
Figure 2.9	Variation of specific growth rate with intensity of light incident on the surface of photobioreactor.	33
Figure 2.10	Variation in concentration of CO ₂ evolved from reactor as the concentration of cells in the reactor volume increase. Study was conducted at 5% (v/v) concentration of CO ₂ and 161.67 mW radiant flux of light.	36
Figure 3.1	Continuously mixed photobioreactor containing the photosynthetic algae <i>C. vulgaris</i> .	41
Figure 3.2	Complete experimental set-up showing the continuously mixed photobioreactor with a incandescent light source, sparger, pump for media flow and flow meter to measure airflow.	42
Figure 3.3	Variation in radiant flux incident on the surface of the bioreactor with distance from the bioreactor.	43
Figure 3.4	Scan of light irradiance from the luminescent bulb.	43
Figure 3.5	Dry weight calibration curve for Shimadzu model 1240 spectrophotometer at 620 nm.	45
Figure 3.6	Schematic drawing of the grid on a Petrov-Hauser counting chamber. (Brown, 2009)	46

Figure 3.7	Microscopic view of <i>C. vulgaris</i> cells on a Petrov-Hauser counting chamber.	47
Figure 3.8	Transient changes in dry cell weight of <i>C. vulgaris</i> at a dilution rate of 0.01 h^{-1} , 5% (v/v) CO_2 concentration and 93.415 mW radiant flux.	49
Figure 3.9	Transient changes in dry cell weight of <i>C. vulgaris</i> at dilution rate of 0.005 h^{-1} , 15% (v/v) CO_2 and 119.225 mW radiant flux.	49
Figure B.1	Schematic diagram of the photobioreactor.	69
Figure C.1	Experimental set-up used for Soxhlet extraction.	71

LIST of ABBREVIATIONS

ADP	Adenosine Diphosphate
APHA	American Public Health Association
ATP	Adenosine Triphosphate
DC	Direct Current
DNA	Deoxyribonucleic Acid
L: D	Light: Dark
LED	Light Emitting Diode
MFC	Microbial Fuel Cell
NADPH	Nitrogen Adenosine Diphosphate Hydrogen
NADPH ₂	Nitrogen Adenosine Diphosphate Dihydrogen
P _i	Inorganic Phosphate
RNA	Ribonucleic Acid

NOMENCLATURE

μ	Specific growth rate	h^{-1}
S	Substrate concentration	mg/L
K_s	Half saturation constant	mg/L
μ_{\max}	Maximum specific growth rate	h^{-1}
X	Biomass concentration	mg dry weight / L
OD_{620}	Optical density of sample measured at 620 nm	
C	Number of cells counted in the Petrov Hauser counter	
V	Volume of each square on the Petrov-Hauser counter	mL
F	Number of squares counted on the Petrov –Hauser counter	
E_{664}	(Optical density of filtrate at 664 nm) – (Optical density of filtrate at 750 nm)	
E_{665}	(Optical density of acidified filtrate at 665 nm) – (Optical density of acidified filtrate at 750 nm)	
V_1	Volume of 90% acetone used in extraction	mL
V_2	Volume of water filtered	L
L	Pathlength of cuvette used	cm
D	Dilution rate and reciprocal of residence time	h^{-1}
μ_{net}	Net specific growth rate	h^{-1}
$\mu\text{Es}^{-1}\text{m}^{-2}$	Micro Einstein per second per square meter	

1.0 INTRODUCTION

1.1 MOTIVATION FOR BIOCAPTURE OF CARBON DIOXIDE

Increasing concerns about global warming and greenhouse gas emissions has necessitated efficient methods of carbon sequestration. Although natural processes account for 50% of the removal of CO₂ emissions, man-made methods for carbon fixation is still a major issue (Benemann, 2001). A major challenge in sequestering carbon dioxide is the disposal or utilization of the isolated CO₂. High disposal and operating costs render the non-biological methods of carbon fixation an extremely costly affair. An alternative to conventional methods is to use photosynthetic microorganisms for capture of CO₂. About 10% of atmospheric carbon dioxide is utilized through natural photosynthesis every year (Govindjee and Whitmarsh., 1999). The unique ability of microalgae to utilize light energy and CO₂ sets them apart from other microorganisms. Algae are microorganisms that have high abundance in the ecosystem due to their high tolerance levels to various environmental stresses (Fogg, 2001). Photosynthetic algae, such as *Chlorella vulgaris*, have been studied extensively over the years as a candidate for biocapture of CO₂ (Kleinheinz and Keffer., 2002; Yanagi *et al.*, 1995). The *Chlorella* sp. is widely preferred for carbon sequestration due to their tolerance for high levels of carbon dioxide and higher efficiency in utilizing CO₂ through photosynthesis compared to terrestrial plants.

Microalgae such as *Chlorella* sp. are known to have various other uses such as treatment of wastewater, production of biodiesel, production of electricity using microbial fuel cells, animal food supplements and providing valuable extracts for chemical products (Becker, 2004; Barsanti and Gualtieri, 2006; Chisti, 2007; Powell *et al.*, 2009b). A winning approach to the issue of carbon sequestration would be to combine the benefits of carbon fixation by microalgae with any of the aforementioned technologies. One such innovative method for carbon sequestration developed by Powell *et al.* (2009b) uses photosynthetic algae *C. vulgaris* at the

cathode of a complete microbiological fuel cell. This novel microbial fuel cell was constructed to operate as a carbon dioxide neutral microbiological power generator.

However, a major setback in the scale-up of this complete microbial fuel cell, was the growth rate of the algal species used. Carbon dioxide, a major substrate for photosynthesis greatly influences the growth rate of photosynthetic algae. Also, both the intensity of the light incident on the reactor surface and the wavelength available for photosynthesis affect growth rate (Barsanti and Gualtieri, 2006). Studies by Powell *et al.* (2009a) showed that the growth rate of *C. vulgaris* cells is dependent on the interacting effect of light intensity and CO₂. It was proven that for a specific concentration of CO₂, the amount of light supplied was the limiting factor on the growth rate of *C. vulgaris* (Powell *et al.*, 2009a). Hence, this research project was instigated with the objective of maximizing growth of *C. vulgaris*. Another objective was to study the effects of light intensity and CO₂ on the specific growth rate of *C. vulgaris*.

An innovative photobioreactor design can augment growth rates of the microalgae and reduce production costs considerably. In this research project, the effect of light intensity on the growth of the photosynthetic algae *C. vulgaris*, in a novel circulating loop photobioreactor is investigated. External loop airlift bioreactors have been proven suitable for most biological processes due to its adaptability to 3-phase applications, absence of any moving parts and good mixing efficiency (Nikakhtari and Hill, 2005). Also used was an externally illuminated continuous flow mixed reactor to study the interacting effects of light intensity, concentration of carbon dioxide and flowrate of nutrient medium. Use of this closed system allowed for minimum contamination of the culture in the reactor and easy control of culture parameters such as pH, oxygen, carbon dioxide concentration, and temperature (Barsanti and Gualtieri, 2006).

1.2 LITERATURE REVIEW

1.2.1 Microbial Growth Kinetics

The relation between the specific growth rate (μ) of a population of microorganisms and the substrate concentration (S) is a valuable design tool in biotechnology. This relationship is represented by a set of theoretical models that describe the behavior of a microbial system. The classical models, which have been applied to microbial population growth, include the Verhulst and Gompertz function. Several microbial growth and biodegradation kinetic models have been developed such as Monod's, Andrew's, Bungay's weighted model, general substrate inhibition models and sum kinetic models (Okpokwasili and Nweke, 2005). However, the idea of microbial growth kinetics has been long dominated by a model originally proposed by Monod in 1942. For years, the Monod model has been tried and tested by a large number of researchers (Bailey and Ollis., 1986). The Monod model introduced the concept of a growth limiting substrate.

$$\mu = \frac{\mu_{\max} [S]}{K_s + [S]} \quad (1.1)$$

Where μ = specific growth rate,

μ_{\max} = maximum specific growth rate,

S = substrate concentration,

K_s = half saturation constant (i.e. substrate concentration at half μ_{\max}).

In Monod's model, the growth rate is related to the concentration of a single growth-limiting substrate through the parameters μ_{\max} and K_s (Okpokwasili and Nweke, 2005). The Monod model is often compared to the Michaelis –Menten model for enzyme kinetics. This shows that the growth of microbes is dependent on a single growth limiting substrate just as the activity of an enzyme is dependent on the substrate concentration.

Microbial growth phases. The growth of a microorganism follows different phases. These phases were studied by introducing a culture of microorganisms into a batch reactor

containing nutrient medium. The time required to pass through the various phases would depend on the initial cell concentration, concentration and constituents of the nutrient medium, pH and temperature, among various other factors (Bailey and Ollis, 1986). The type of growth depicted in Figure 1.1 is characteristic of the growth kinetics observed in a batch cultivation of microorganisms. Figure 1.1 shows the increase in the number of cells in the batch reactor with respect to time.

Phase A is the initial phase and is called the lag phase. During this phase, the microbial cells inoculated into the bioreactor are getting accustomed to the medium. The cells are in a state of producing the enzymes required for utilizing components of the new medium in their metabolic pathway. Also, new proteins and other molecules such as the DNA and RNA required for cell multiplication are being developed. Hence, in the lag phase, there is no significant change in the cell number. It is only towards the end of the lag phase that a minor change in the biomass concentration is usually noticed. For most of the lag phase, the change in number of cells per unit volume of the media is zero (Lee, 1992). Following the lag phase is a period of exponential or logarithmic growth; phase B. During this phase, the cells have already got accustomed to the media and have started utilizing the sugars present in their metabolic pathway. In this phase, the cells have also started to multiply and produce daughter cells. This leads to an increase in the biomass concentration. The slope of the exponential phase is used as a measure of the specific growth rate of the microorganism (Najafpour, 2007).

It has been observed in previous studies that the growth rate of the cells increase exponentially with time during the exponential phase (Bailey and Ollis, 1986). Towards the end of this phase, a stage is reached when the rate of division of the cells has reached its maximum value but the biomass loading may continue to increase. This implies that the cells have stopped multiplication but the existing cells continue to grow in size. This phase is called the Stationary phase; phase C. At the end of this phase, a number of cells begin to die leading to a decrease in the cell number and the growth rate. The cells now enter the final phase of growth, the death phase (phase D). In the death phase, the number of living cells present in the media continues to decrease until the end of this phase.

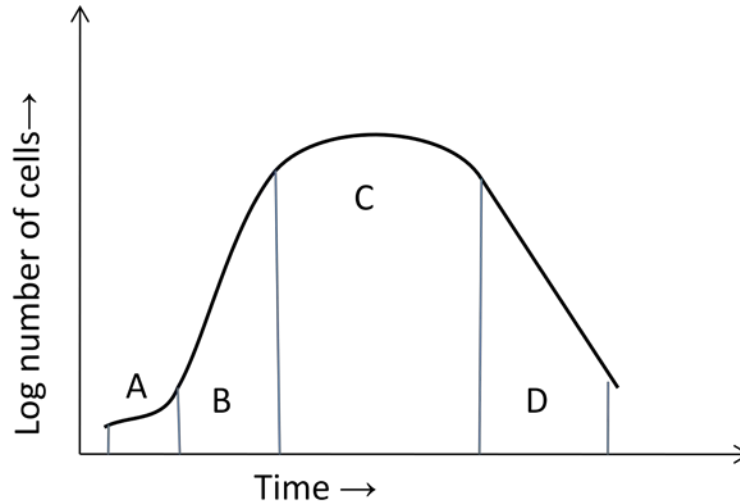


Figure 1.1 Typical growth curve for batch cell cultivation. The growth of the microbe follows the various phases; lag phase (A), exponential growth phase (B), stationary phase (C) and death phase (D). (Bailey and Ollis, 1986)

1.2.2 Growth of *Chlorella vulgaris*

Growth of photosynthetic algal cells depends on a number of factors including the intensity of light available for photosynthetic reactions, concentration of CO₂, temperature, pH and mixing characteristics in the reactor.

Light. The effect of light is dependent upon two factors; intensity of light that is incident on the surface of the reactor and the presence of light and dark phases. The intensity of light available is in some cases expressed as the average irradiance per algal cell. At lower light intensities, the ratio of oxygen to carbon dioxide plays a significant role. When the concentration of oxygen is higher at a lower light intensity, the process of photosynthesis is replaced by photorespiration. At higher light intensities greater than 5-10% of full daylight (2000 $\mu\text{Es}^{-1}\text{m}^{-2}$), the cells undergo photoinhibition (Barsanti and Gualtieri, 2006).

C. vulgaris has preferable action spectra in the absorption ranges: blue (420 - 450 nm) and red (660 – 700 nm) (Lee and Palsson, 1996; Matthijs *et al.*, 2007). Hence, light used for all experiments in this research have been selected to provide energy within this spectrum. Although

a number of light sources may be used for growing algae, the most commonly used are fluorescent lamps and light emitting diodes. Both these types are cost effective, have a low heat output, and are extremely efficient and stable (Geider and Osborne, 1992).

Presence of light and dark phases is of high significance in case of photosynthetic algae such as *C. vulgaris*. Efficient growth of algal cells is ensured by maintaining a light and dark phase in the photobioreactor as photosynthesis comprises light dependent and light independent reactions.

Carbon Dioxide. The dissolved CO₂ levels in the reactor solution have a direct effect on the growth rates of *C. vulgaris* cultures. CO₂ is a major participant in light independent reactions of photosynthesis (Barsanti and Gualtieri, 2006). *Chlorella* sp. has been found to survive in atmospheres containing 0.03 to 40% CO₂ (Hirata *et al.*, 1996). Powell *et al.* (2009a) showed that a CO₂ concentration of 10% by volume in the air bubbled through the reactor is ideal for *C. vulgaris* cultures.

Temperature. *Chlorella* sp. has been found to have an optimum temperature range 10-30°C with *C. vulgaris* cultures having a preferred range of 20°C - 30°C (Hirata *et al.*, 1996).

pH. *C. vulgaris* cultures have an optimum pH range 5.5 to 7.0. Studies by Powell *et al* (2009a) showed that variations in pH over this range had a minimal effect on the growth rates of *C. vulgaris*.

Mixing. Proper mixing in the reactor is required to prevent sedimentation, avoid thermal stratification and improve gas exchange between culture and air. Use of photobioreactors fitted with spargers or bubblers enhances mixing characteristics.

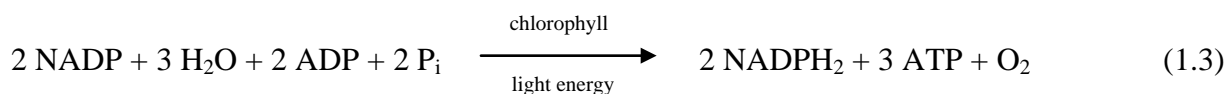
1.2.3 Algae and Photosynthesis

“Photosynthesis can be defined as the physico-chemical process by which photosynthetic organisms use light energy to drive the synthesis of organic compounds” (Govindjee *et al.*, 1999). The process of photosynthesis is essential for the sustenance of life on Earth. Photosynthesis converts the energy of the sunlight into reduced carbon and oxygen. Since the evolution of oxygen is involved, the aforementioned process is also known as oxygenic photosynthesis. Photosynthesis by macroalgal species account for 50% of photosynthetic processes globally (Geider and Osborne, 1992). The process of photosynthesis is dependent upon the intensity of light that is available for utilization. This is defined as the irradiance or the quantity of light that is incident on a surface and is expressed in terms of Watts per square meter (W/m^2).

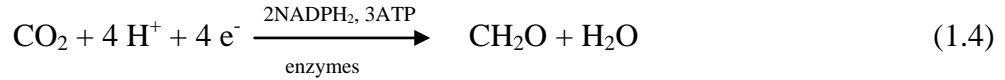
Photosynthesis comprises of two significant steps: the light phase reactions and the dark phase reactions. As the name indicates, light phase reactions occur in the presence of light while dark phase reactions take place in the absence of light. The overall equation for photosynthesis is given by (Fogg, 1954):



Light dependent reactions. In the presence of photosynthetic pigments, present on the thylakoid membrane inside a photosynthetic cell, light energy is converted into chemical energy. Energy of the sunlight is converted to a biochemical reductant NADPH_2 (nitrogen adenosine diphosphate dihydrogen) and a high energy compound ATP (adenosine triphosphate) (Masojidek *et al.*, 2004). The main objective of the light dependent reactions is to convert available light energy into a form that can be used readily in metabolic processes. The reaction for the light dependent phase can be given as (Masojidek *et al.*, 2004):



Light independent reactions. The dark phase reactions involve the utilization of the NADPH₂ and ATP molecules produced by the light dependent reactions. These reactions occur in the stroma and they represent the process of carbon fixation. The reaction for the light independent phase is given as:



Significance of Light - Dark Cycle. While the light independent reactions of photosynthesis are responsible for carbon fixation, the energy for this process is obtained from the light dependent reactions. Hence, both steps of photosynthesis are essential to obtain a high growth rate of algal cells and maximum utilization of carbon dioxide. In the dark phase, respiration and pending light independent reactions occur (Geider and Osborne, 1992). Maximizing growth rate of a photosynthetic organism depends largely on determining the right balance between light and dark phase reactions. The duration of light and dark phases required varies depending on the photosynthetic species involved. In case of *C. vulgaris*, the best Light: Dark (L: D) cycle is known to be 16:8. Some algal species have optimum L: D cycles of 14:10 and 12:12 (Barsanti and Gualtieri, 2006).

1.2.4 Algae and Photobioreactors

Photobioreactors are closed systems that provide a protected and controlled environment for algal growth. Photobioreactors are ideal for attaining higher cell density of microalgal cultures. This configuration allows control of input parameters such as pH, temperature, concentration of nutrient medium, oxygen and carbon dioxide concentration. Different modes of culture can be used for cultivation of microalgae. The most commonly used modes are batch, continuous and immobilized cultures (Lee and Shen, 2004). The mode of culture may be decided by the researcher based on the output parameters to be studied.

Use of Circulating Loop Photobioreactor in Fed Batch Mode. Fed-batch cultures are essentially a combination of batch and continuous cultures. In fed-batch cultures one or more substrates may be continuously or semi-continuously fed to the culture. This will prevent growth

limitations due to the substrate that is supplied and consequently enhance the growth rate of the culture (Shuler and Kargi, 2002). Fed batch systems are useful in studying the dependence of growth rates on individual parameters.

In this research, a circulating loop airlift photobioreactor as shown in Figure 2.1 was used to study the individual effect of light intensity on growth rate of the algae *C. vulgaris*. Airlift photobioreactors are usually used for processes where two-phase systems are involved. Airlift systems are cost effective, have a simple mechanical configuration and superior mixing properties (Bailey and Ollis, 1986). Airlift photobioreactors with external loop configuration are commonly used in biological processes. The external circulating loop allows for a lower overall gas holdup and thereby enabling proper liquid circulation and efficient mixing in the reactor (Chisti, 1989).

Use of a Continuous Flow Photobioreactor. The use of a continuously mixed reactor allows manipulation of growth rate as an independent parameter and is perfect for the study of the effects of environmental changes on cell physiology (Shuler and Kargi, 2002). In a continuous culture the growth rate is allowed to reach a steady state at which the cell density of the culture remains constant. A further classification of continuous cultures includes turbidostats and chemostats. In turbidostat cultures, the fresh nutrient medium is introduced once the cell density reaches a predetermined point. In a chemostat, there is a constant flow of nutrient medium into the reactor along with removal of an equal amount of the reactor volume. The continuously mixed photobioreactor as shown in Figure 3.1 was used to study interacting effects of light intensity, concentration of CO₂ and flowrate of nutrient medium.

1.2.5 Microbial Fuel Cells

Microbial fuel cells (MFCs) were first discovered in the year 1912. However, until recent years, MFCs have not been extensively studied. The recent developments in the field of MFC's have made it an interesting source of electricity. Microbial fuel cells produce electricity by taking advantage of the oxidation reduction reactions occurring in a microorganism.

Metabolism of microbiological cells used in MFC. In order to understand the transport phenomenon in a microbiological fuel cell using microalgae, it is important to study the various metabolic processes occurring during the light and dark phase reactions. The metabolic process in a living cell occurs via two pathways; catabolic and anabolic pathway. Anabolism is defined as the use of energy to build cellular structures and catabolism is defined as the breakdown of nutrients into smaller molecules and energy (Bailey and Ollis, 1986).

The catabolic pathway which comprises the light phase reactions involves the Z-scheme which is an electron transport chain (Masojidek *et al.*, 2004). These light reactions occur on the thylakoid membrane within the cell. The major participants in the light reactions are Photosystem I and Photosystem II. The overall reaction for the Z-scheme is as represented in Equation 1.3. The energy produced by the Z-scheme is utilized by carbon assimilation in the dark phase reactions. The fixation of carbon dioxide occurs via the Calvin-Benson cycle which is represented by equation 1.4. This reaction occurs in the presence of the Rubisco (ribulose biphosphate carboxylase/oxygenase) enzyme which acts as a carboxylase when the $O_2:CO_2$ ratio is low.

Following the Calvin-Benson is the process of photorespiration. In the presence of a higher $O_2:CO_2$ ratio, the Rubisco enzyme functions as an oxygenase and catalyses the reaction that utilizes oxygen. Hence, at lower concentrations of carbon dioxide the Rubisco tends to favor photorespiration (Barsanti and Gualtieri, 2006).

Classification of MFC's. Microbial fuel cells can be of different types. Classification of fuel cells could be based on the fuel used and the extent to which the microbes are incorporated in the fuel cell.

Based on the source of fuel used for production of electricity, the MFC can be classified as follows:

- Direct fuel
- Indirect fuel

An alternative classification of fuel cells is:

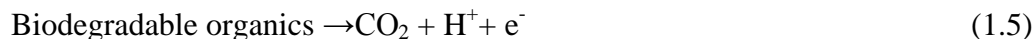
- Microbial fuel cell with a biocathode
- Microbial Fuel Cell with a bioanode
- A complete microbial fuel cell

In a MFC with a biocathode, only the cathodic half of the cell is microbic. The anodic half of the cell is non- microbic. The commonly used anodic half is a potassium ferrocyanide cell with a graphite/carbon electrode. Similarly in a MFC with a bioanode, only the anodic half is microbic. The third category of MFC, a complete microbial fuel cell, has also not been researched very much except for a few researchers (Powell *et al.*, 2009b).

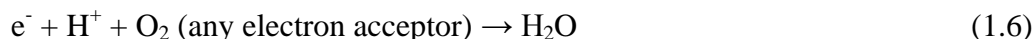
Microbial Anodic Half Cells. Microbial fuel cells with anodic half cells have been well researched over the years. Most researchers of microbial fuel cells focus on the anodic part of the fuel cell. Researchers have modified and optimized the growth of microbes at the anodic half of a MFC.

A typical MFC with microbial anode is shown in Figure 1.2. The electrons produced by the microbial metabolic reactions are captured by mediator molecules and taken to the anode. These electrons travel through an external circuit to the cathode where they are accepted in the cathodic reactions. The reactions occurring in this MFC are as listed below (Mohan *et al.*, 2008):

Anode:



Cathode:



Microbial anodic half cells have been used in biosensors for determination of biological oxygen demand (BOD) and bioelectricity production from wastewater.

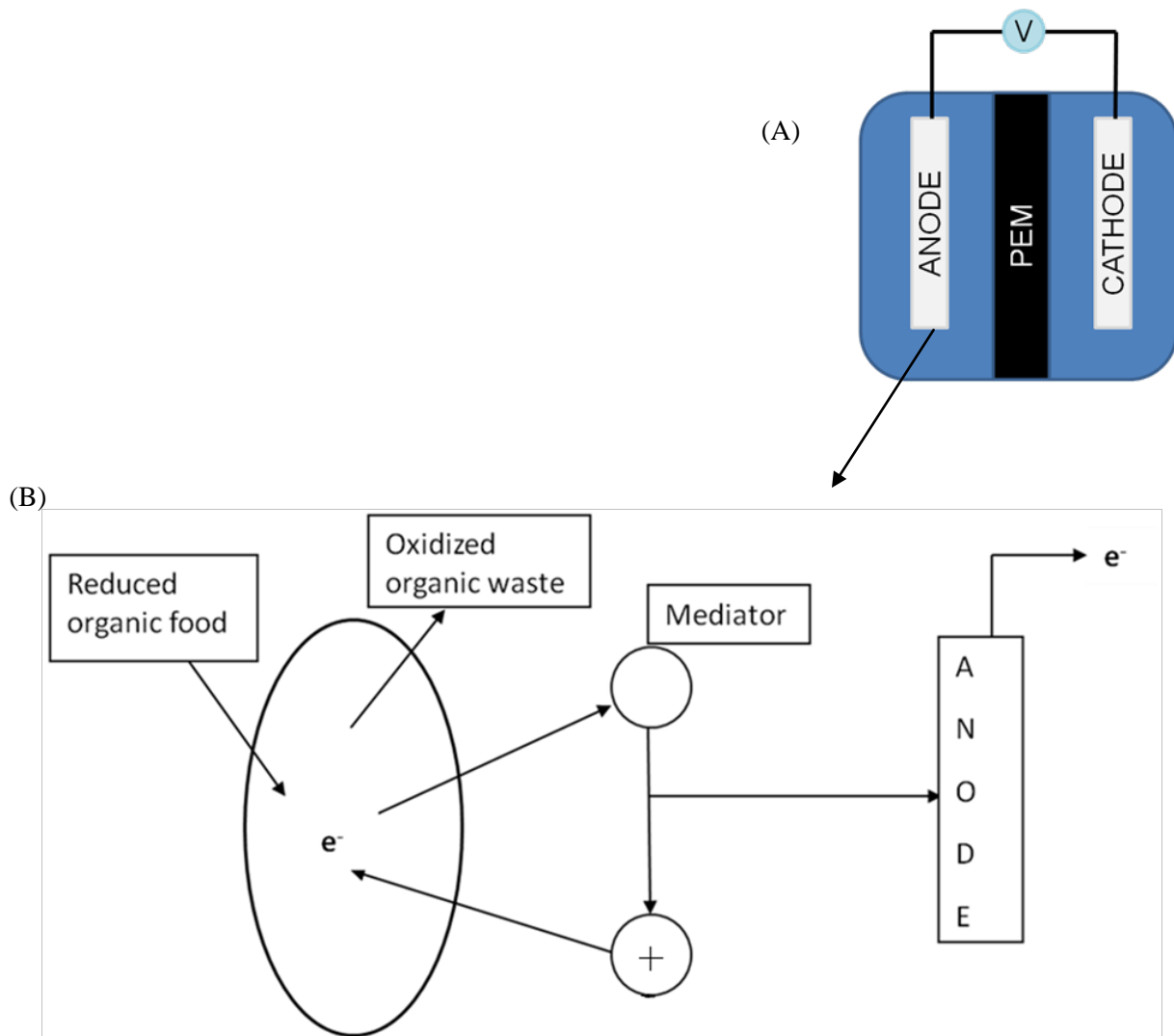


Figure 1.2 (A) A typical microbiological fuel cell with the essential components; anode, cathode, a proton exchange membrane and an external circuit connecting the two electrodes. (B) Schematic showing the processes occurring at the anode. Electrons produced due to the metabolic reactions in the cell are captured by mediator molecules to the anode, which then moves along the external circuit to produce current. (Powell *et al.*, 2009b)

Microbial Cathodic Half Cells. In conventional MFC's an abiotic cathode is used. Gregory *et al.* (2004) demonstrated that bacteria can take up electrons from a graphite electrode without hydrogen as an intermediate electron shuttle.

In an MFC with a microbial cathode, only the cathodic half uses microbes. The anodic half of this fuel cell is abiotic. This type of fuel cell has been studied by only a few researchers. Many more studies will be required to optimize the growth of microbes at the cathodic half of the cell. Clauwaert *et al.* (2007a) studied the use of an open air Biocathode in a MFC. A continuously wetted cathode with microorganisms that act as biocatalysts for oxygen reduction was used in the MFC. Powell *et al.* (2009a) studied the use of *C. vulgaris* as a cathodic half cell wherein nutrient broth containing *C. vulgaris* at the cathode was connected to anode where ferrocyanide was oxidized to ferricyanide. Figure 1.3 shows the use of algal cells at the cathode.

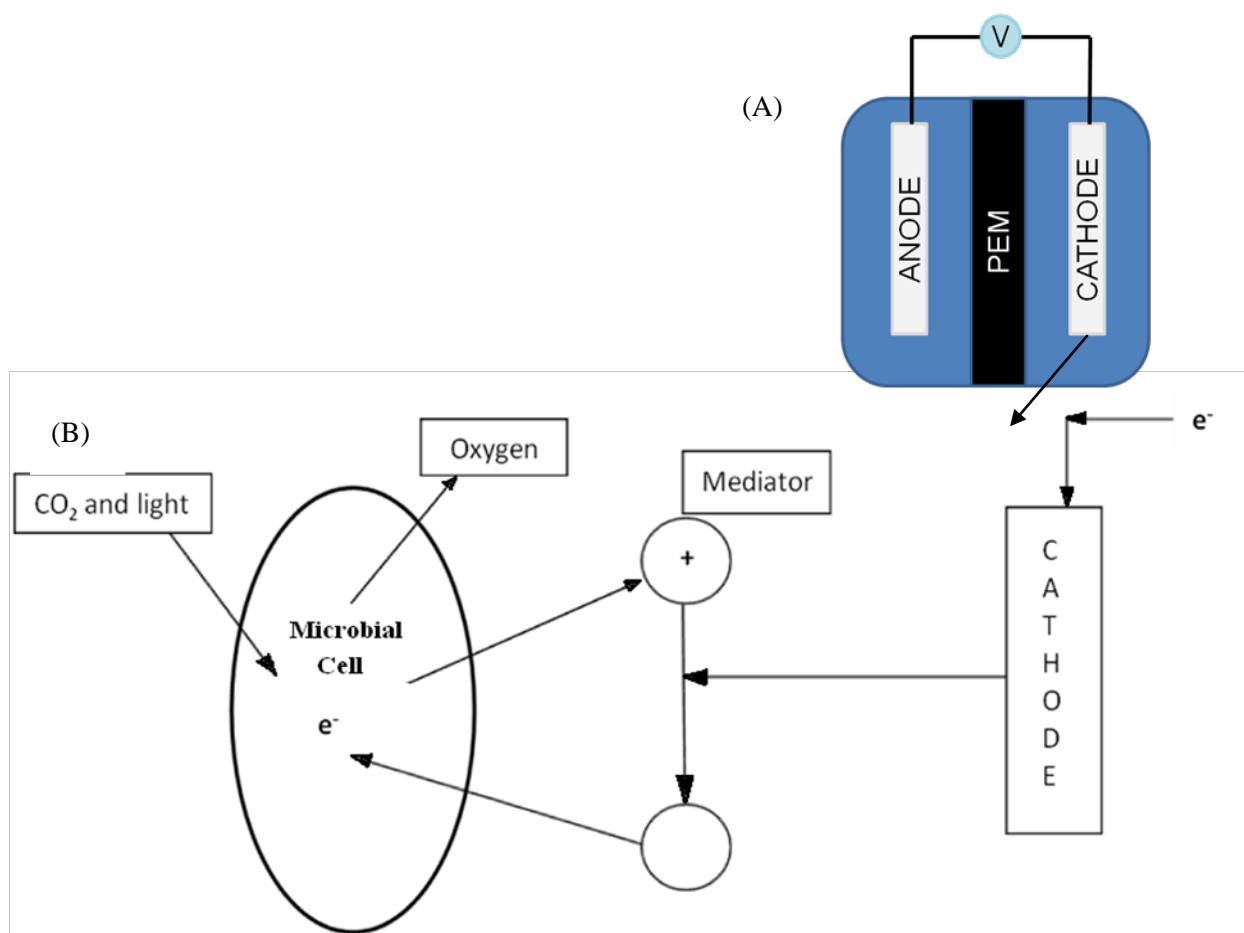


Figure 1.3 (A) A typical microbiological fuel cell with the essential components; anode, cathode, a proton exchange membrane and an external circuit connecting the two electrodes. (B) Schematic showing the processes occurring at the cathode. Electrons from the anode are used to run the metabolic reactions of the microbes at the cathode. (Powell, *et al.*, 2009b)

The reactions occurring at the cathodic half of the MFC can be represented as follows (Powell *et al.*, 2009b):

Cathode:



The reactions at the anode would depend upon the type of electrolyte and electrode used at the anodic half of the MFC. In the work of Powell *et al.* (2009a), the anodic half cell was potassium ferrocyanide/ ferricyanide.

Complete Microbial Fuel Cells. These microbial fuel cells are the least researched category of MFCs. The same groups of researchers working on MFC with microbial cathodes have initiated work on complete microbial fuel cells. In a complete microbial fuel cell, the micro-organisms drive both the anodic and the cathodic reactions.

A research group led by Clauwaert (2007b) studied a MFC in which microorganisms in the cathode performed a complete denitrification by using electrons supplied by microorganisms oxidizing acetate in the anode. The current production was found to be proportional to the denitrification rate. The open cell voltage was found to be typically between 0.300 V and 0.360 V when nitrate was being supplied to the cathodic system.

In a study by Prasad *et al.* (2006), two configurations of fuel cells were used. In the first configuration, a microbial anode was connected to an abiotic cathode. In the second configuration, a complete microbial fuel cell was used. On comparison of the two configurations, the second configuration was found to be more efficient.

Configuration 1: Graphite or graphite felt | *Clostridium sp.*+ deaerated nutrient broth || ferricyanide | graphite.

Configuration 2: Graphite or graphite felt | *Clostridium sp.* + deaerated nutrient broth || *Thiobacillus ferrooxidans* + nutrient broth | graphite.

Studies showed that in configuration 1, the ferricyanide in the cathode compartment becomes depleted with time. It has to be replaced often during the course of the experiments. On the other hand, in the configuration 2, the ferric sulfate present in the nutrient broth of the microbial cathode compartment acts as the electron acceptor and is continuously regenerated by the micro-organisms and hence the solution in the compartment remains clear, unlike the case of ferricyanide. Hence, the reactions at both the electrodes were driven entirely by microorganisms.

Another study by Powell *et al.* (2009b) involved building a complete MFC with yeast at the anode and algae at the cathode. This study developed a ground breaking microbial fuel cell which was carbon dioxide neutral and produced valuable by-products such as ethanol, algal biomass and chlorophyll. The cathodic half of the microbial fuel cell used a photosynthetic culture of *C. vulgaris* while the anodic half consisted of a yeast fermentation culture of *Saccharomyces cerevisiae*. A power density of 0.95 mW/m^2 and an open circuit potential of 0.350 V was obtained. It was observed that the yeast cells grew at a significantly higher rate compared to the microalgae. This was a major limiting factor in achieving higher power densities. In conclusion, the energy capture efficiency of the MFC could be maximized by increasing the growth rate of *C. vulgaris*.

1.2.6 Use of Algae in Microbial Fuel Cells

Algae are versatile microorganisms that can survive in harsh conditions and adapt to different types of substrates such as CO_2 and wastewater. Algal species such as blue-green algae *Anabaena*, macroalgae *Ulva lactuca*, green alga *Chlamydomonas reinhardtii* and *C. vulgaris* have been used successfully in MFC's that can produce energy capture efficiencies of up to 50% (Velasquez-Orta *et al.*, 2009; Lam *et al.*, 2003; Rosenbaum *et al.*, 2005; Powell *et al.*, 2009a; Powell *et al.*, 2009b). Use of microalgae in MFC for energy production is significant due to operation at low temperatures and continued power generation even during a dark period i.e. in the absence of light. With the use an efficient photobioreactor design, high production rates of algae can be obtained. Consequently, increased power densities can be expected.

1.3 KNOWLEDGE GAP AND SCOPE FOR WORK

Use of microalgae in environmental biotechnology has been studied extensively over the years. But the combination of these technologies to obtain a highly competent process has not been given much importance. In recent years, many researchers concentrated on studying the potential of combining wastewater treatment with biocapture of CO₂ using photosynthetic algae. Although this combination has proven successful, a number of concerns still exist.

On the other hand, the use of photosynthetic algae for energy production coupled with biofixation of CO₂ is relatively new. Much more detailed analysis will be required to assess the potential of this process. Bioelectricity production using algae in MFCs is useful as a method of power generation, but it needs to be further improved in order to make it competitive with alternative energy technologies (Velasquez-Orta *et al.*, 2009).

Scope for work. The overall objective of this research project is to maximize growth of *C. vulgaris* cells in a novel circulating loop photobioreactor intended for future use as cathode in a complete microbial fuel cell. This research project is carried out as an extension to the work done by Powell *et al.* (2009b) on the first carbon dioxide neutral complete microbial fuel cell. The studies carried out by Powell *et al.* proved the feasibility of this microbiological fuel cell as an energy production device. It was hypothesized that an efficient bioreactor design could enhance outputs of this fuel cell, hence, necessitating a novel circulating loop bioreactor that will maximize the growth of *C. vulgaris*. The specific objectives of this research are:

- Use of the novel circulating loop photobioreactor operated in fed-batch mode to study the effect of light intensity on the specific growth rate of *C. vulgaris*.
- Study of effects of light and dark phase in the circulating loop photobioreactor on the specific growth rate of *C. vulgaris*.
- Study of effects of CO₂ concentration in the circulating loop photobioreactor on the specific growth rate of *C. vulgaris*.

- Study of interacting effects of light intensity at varying concentrations of carbon dioxide and flowrate of nutrient medium in a continuous flow mixed reactor on the specific growth rate of *C. vulgaris*; and
- Analyze the variations of light intensities and concentration of carbon dioxide to maximize the growth of *C. vulgaris*.

1.4 DESCRIPTION OF FOLLOWING CHAPTERS

Chapter 2 will discuss use of the circulating loop photobioreactor to study individual effects of light intensity and CO₂ concentration on the specific growth rate of *C. vulgaris*. This chapter includes the pattern of CO₂ utilization by the photosynthetic algae *C. vulgaris* in the circulating loop photobioreactor. Biomass yield of *C. vulgaris* measured using sealed glass bulbs have also been included in this chapter.

Chapter 3 will discuss use of an externally illuminated continuous flow mixed photobioreactor to study the interacting effects of light intensity at varying concentrations of carbon dioxide and flowrate of nutrient medium on the specific growth rate of *C. vulgaris*.

Finally, Chapter 4 will conclude the results shown in chapters 2 and 3. Recommendations for future work will also be mentioned in this chapter.

2.0 EFFECT OF LIGHT INTENSITY AND CO₂ ON GROWTH OF *Chlorella vulgaris* IN A NOVEL CIRCULATING LOOP PHOTOBIOREACTOR

2.1 INTRODUCTION

Airlift reactors are versatile systems that are often used for two-phase or three-phase biological processes. Previous studies (Siegel *et al.*, 1986) have proven the successful use of airlift bioreactors for the growth of microbial cells. An airlift reactor may be defined as “a pneumatically agitated system characterized by fluid circulation in a defined cyclic pattern through channels built specifically for this purpose” (Siegel and Merchuk, 1988). The main requisites for a photobioreactor used for growing microalgae are effective distribution of light through the entire reactor volume, efficient gas mass transfer and proper mixing.

Taking these factors into consideration, the novel circulating loop airlift photobioreactor was developed for growing the photosynthetic algae *C. vulgaris*. Airlift systems provide superior mixing and gas mass transfer rates compared to traditional bubble column or stirred tank bioreactor models as demonstrated by Merchuk *et al.* (2000), Chisti (1989) and Nikhaktari and Hill (2005). Light distribution is a major factor affecting the productivity of the algal cells. Uniform distribution of light can be achieved by use of superior designs of photobioreactors (Morita *et al.*, 2000). The novel circulating loop photobioreactor is one such advanced design that enhances light distribution in the reactor volume. Hence, higher growth rates of algal cells are easily achieved. Another important aspect that can affect the operation of an external loop airlift bioreactor is the design of the gas-liquid separator. Many studies conducted with external loop airlift bioreactors have shown that inefficient design of the gas separator could lead to fluctuations in liquid velocity (Merchuk and Siegel, 1988). This limitation was overcome in the novel circulating loop photobioreactor by having the region of gas separation open to the

atmosphere. Such a configuration ensured the complete separation of gas from liquid before entry into the downcomer column.

The main objective of this part of the research project was:

- To study the effect of light intensity on the specific growth rate of *C. vulgaris*
- To study of effects of CO₂ concentration on the specific growth rate of *C. vulgaris*; and
- To study of effects of light and dark phase in the circulating loop photobioreactor on the specific growth rate of *C. vulgaris*.

2.2 EXPERIMENTAL SETUP AND PROCEDURES

2.2.1 Photobioreactor

Specifications of photobioreactor. The novel circulating loop photobioreactor is shown in Figure 2.1. Table 2.1 enlists the specifications of the circulating loop photobioreactor. It may be noted that the ratio of the diameter of downcomer column to that of the riser column is 0.75. The average circulation velocity was measured based on the average time required for completing one loop length of the reactor.

Table 2.1 Specifications of the circulating loop photobioreactor

Inner diameter of riser section (m)	0.0508
Inner diameter of downcomer section (m)	0.0381
Loop length (m)	3.058
Average circulation velocity (m/s)	0.12
Average circulation time (s)	26.5
Working volume (Litres)	4.63
Number of orifices in sparger	12
Gas holdup in riser column	0.0045

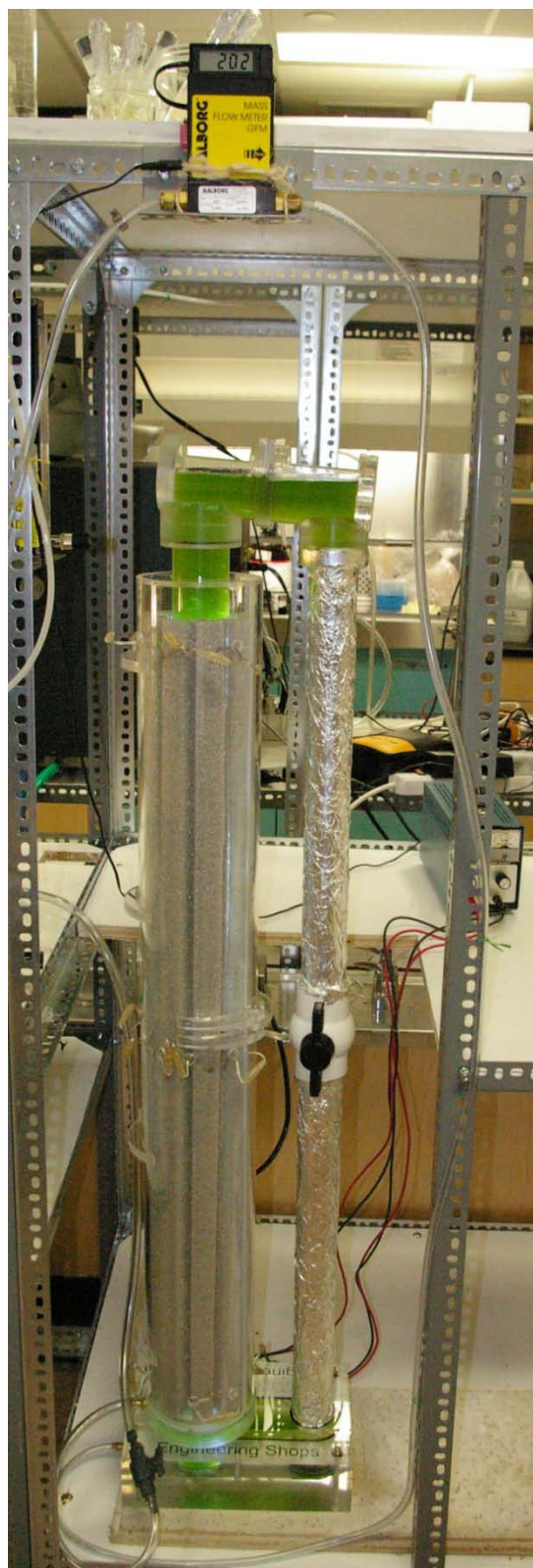


Figure 2.1 Novel circulating loop photobioreactor containing the photosynthetic algae *C. vulgaris* operating in fed-batch mode

Material of Construction. The photobioreactor was constructed of acrylic which is a common material of construction for most research photobioreactors due to its superior qualities. This material is transparent, light, strong and easy to work with. Also, acrylic provides all the advantages of glass and is more flexible (Behrens, 2005).

Illumination of the photobioreactor. The photobioreactor was equipped with 16 strips of white light emitting diodes (LED) on the outside surface of the riser column. Figure 2.2 shows the schematic diagram of 1 LED strip. LED lights are known to have an 80% electrical efficiency and produce light with a spectrum matching the absorption spectra of *C. vulgaris* (Javanmardian and Palsson, 1991). The action spectra of *C. vulgaris* show preferred absorption ranges: blue (420 - 450 nm) and red (660 – 700 nm) (Lee and Palsson, 1996; Matthijs *et al.*, 2007). The irradiance profile for a single LED bulb is shown in Figure 2.3. The spectrum of LED lights is mainly in the preferred absorption ranges for *C. vulgaris*. However, the irradiance available in the red region is limited. The specifications of the LED lights used in this photobioreactor are listed in Table 2.2.

In all runs, a light phase was maintained in the riser and dark phase was maintained in the downcomer as shown in Figure 2.4. While the riser was lit with LED lights, the downcomer column was covered with light blocking material. *C. vulgaris* requires an L: D (Light-Dark) cycle of 16:8 (Barsanti and Gualtieri, 2006). This ratio was incorporated into the design of the photobioreactor since the volume of riser column to that of the downcomer was 2:1.



Figure 2.2 Schematic of LED Strip. Each strip is 1.0 m in length and has 60 bulbs in total.

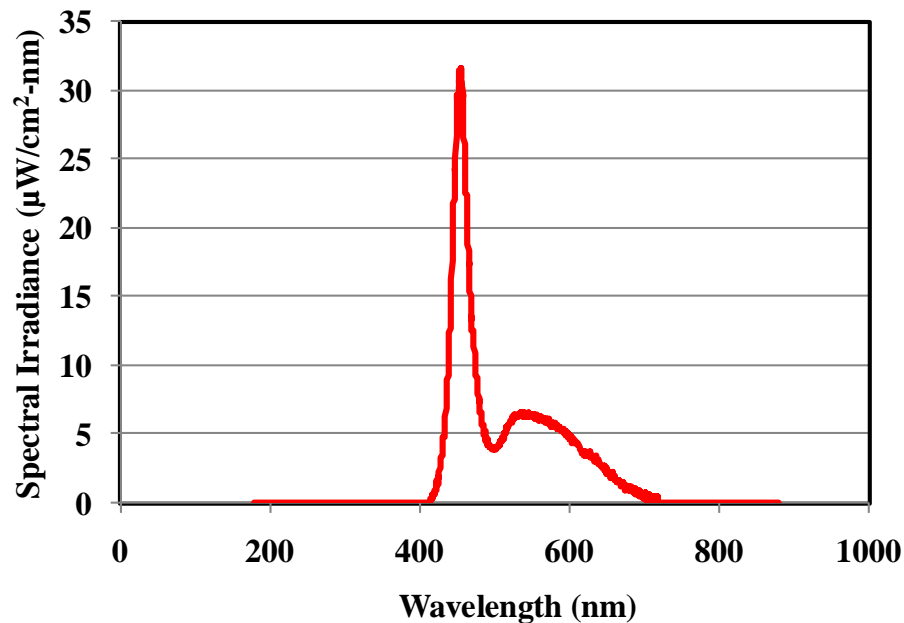


Figure 2.3 Scan of light irradiance from the LED bulb.

Table 2.2 Specifications of LED lights used for the circulating loop photobioreactor

Length of each strip of LED (cm)	100.58
Number of LED bulbs on each strip	60
Colour of LED	White
Maximum voltage requirement (V)	12
Operation Temperature (°C)	10 - 40
Current requirement per strip (mA)	20
Watts emitted by each strip (W/m)	4.8



Figure 2.4 Light and dark phases maintained in the circulating loop photobioreactor illuminated with LED lights

Mixing of reactor volume. Efficient circulation of algal culture was ensured with the use of air spargers. Airflow causes the culture medium to circulate and was supplied to the photobioreactor via a flowmeter through a stationary sparger fitted at the bottom of the riser column. Studies by Powell *et al.* (2009b) showed that variation in pH had no effect on the growth of *C. vulgaris*. As such, fresh sterile modified BOLD's media with a pH of 6.8 was used as the culture medium in each batch run.

Circulation. In an airlift reactor liquid circulation occurs due to the differences in density of liquid in the riser and the downcomer columns (Chisti, 1989). Efficient liquid circulation ensures uniform light distribution, temperature, pH and mixing (Behrens, 2005). In the novel

circulating loop photobioreactor the circulation velocity could be varied by changing the height of the liquid in the gas-liquid separator region as shown in Figure 2.5.

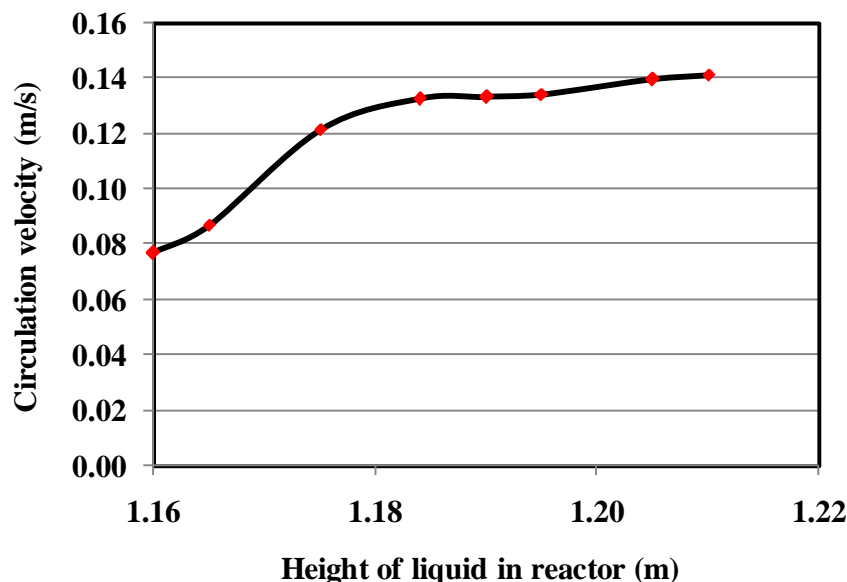


Figure 2.5 Variation in average circulation velocity in the circulating loop photobioreactor with change in height of liquid in the reactor

2.2.2 Experimental studies

Yield of biomass. The typical growth yield of microalgae in a batch reactor was studied at the optimum concentration of 10% (v/v) CO₂ as suggested by Powell *et al.* (2009a). CO₂ is the major carbon source for metabolism in photoautotrophic organisms such as *C. vulgaris*. As such, the biomass productivity of a *C. vulgaris* culture can be obtained by quantifying the amount of CO₂ used by the algae. Biomass yields were determined by measuring the amount of algal biomass produced in a known amount of nutrient media and CO₂ gas in a sealed glass bulb as shown in Figure 2.6. Initial and final values of optical density of the culture in each bulb were used to calculate the yield. The yield of *C. vulgaris* was determined at two specific conditions of dark phase. The two conditions used were; (i) with no dark phase and (ii) with an 8 hour dark phase.

Effect of light intensity. Studies on the growth rate of *C. vulgaris* were performed in this novel photobioreactor operated in fed-batch mode. Variations in the specific growth rate of *C. vulgaris* were noted for various intensities of light. Radiant flux incident on the photobioreactor was varied from 26.945 mW to 431.128 mW.

Effect of light and dark phases. Chisti *et al.* (1999) defines average irradiance as the amount of light that a random cell in the reactor receives. Although *C. vulgaris* requires a light-dark cycle of 16:8, provision of the light or dark phase does not necessarily have to be continuous. Short intervals of the light-dark cycle may also be provided but this is associated with reduced cell productivity (Chisti *et al.*, 1999). In this study, the effect of a continuous dark phase in addition to the short intervals of light-dark cycle was studied. Changes in the specific growth rate of *C. vulgaris* were noted when an additional continuous 8 hour dark phase was provided in the novel circulating loop photobioreactor.

Effect of CO₂ concentration. Earlier studies (Powell *et al.*, 2009a; Yanagi *et al.*, 1995) have shown that *Chlorella* sp. has optimum growth at 10% CO₂. However studies by Powell *et al.* were conducted at a smaller scale and at lower light intensities. Hence, the novel circulating loop photobioreactor which has superior light distribution qualities was used to study the effect of CO₂ concentration on *C. vulgaris* growth. Specific growth rate at 4 different concentrations of CO₂; 0%, 5%, 10% and 15% by volume of the total flowrate of the air and CO₂ mixture entering the photobioreactor were studied. All concentrations of CO₂ mentioned are in addition to the atmospheric concentration of CO₂ (0.03% (v/v)).

Also studied was the pattern of CO₂ usage by algal cells in the circulating loop photobioreactor. In order to study this pattern, the instantaneous concentration of CO₂ evolved from the bioreactor was studied. Gas evolved from the bioreactor was redirected into a glass bulb containing silica beads to absorb moisture. The dry gas then enters the CO₂ sensor which determines the voltage of CO₂ evolved from the bioreactor. The CO₂ sensor used was Vaisala CARBOCAP Carbon Dioxide Module GMM111 in conjunction with the FLUKE 189 True RMS Multimeter which enabled logging of instantaneous data. Figure 2.7 shows the setup used for study of CO₂ evolution from the bioreactor.

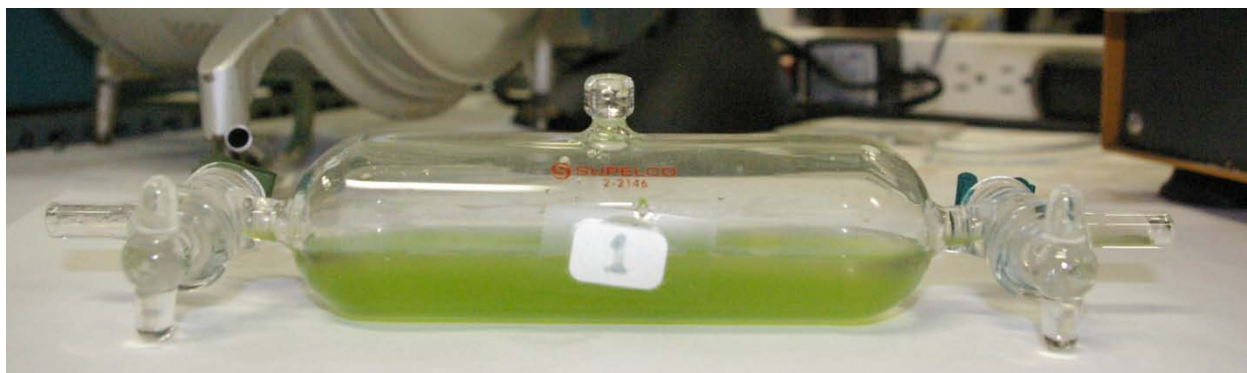


Figure 2.6 Glass bulb used to measure biomass yield of *C. vulgaris*

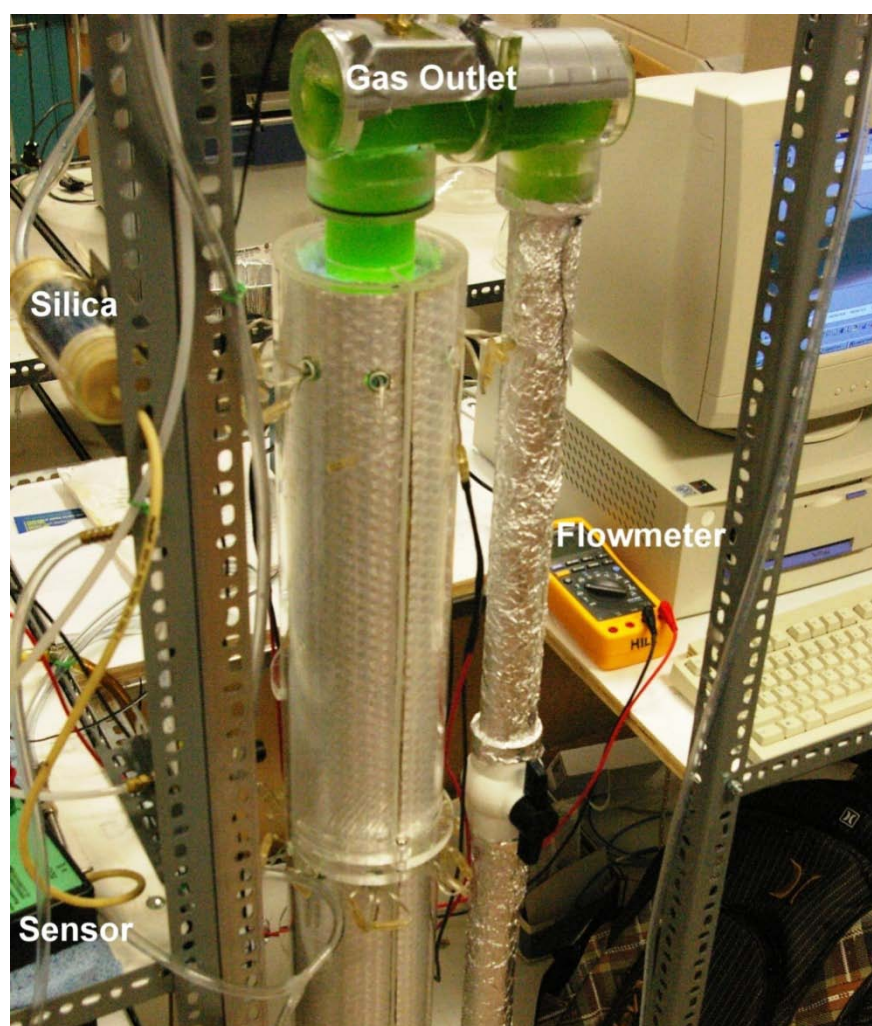


Figure 2.7 Experimental set-up used to study the pattern of CO_2 evolution from the circulating loop photobioreactor containing the photosynthetic algae *C. vulgaris*. The Vaisala CO_2 sensor and FLUKE flowmeter are shown.

Yield of chlorophyll. Chlorophyll content of an algal culture is dependent on the average intensity of light available, nutrient availability, growth phase of the culture and temperature. Measurement of the chlorophyll in a photoautotrophic microorganism defines its photosynthetic rates. Chlorophyll content may be determined through chromatographic, spectrophotometric or spectrofluorometric methods. When the accurate estimation of degradation products of chlorophyll is not required, spectrophotometric methods are used (Porra, 2006). Use of spectrophotometry is also preferred due to the ease and rapidity of the method. Various techniques of spectrophotometric analysis of chlorophyll have been developed. Most techniques involve the use of an organic solvent to extract the chlorophylls from the microbial cells. This is followed by a homogenization step and subsequent analysis of the absorbance of extracted pigments using a spectrophotometer. Most commonly used solvents include 100% acetone, 90% acetone, hot 100% methanol and 1:1 solution of dimethyl sulfoxide and acetone. 90% acetone is highly recommended as it is less toxic (Porra, 2006).

In this research, the standard method APHA 10200H (APHA, 1999) was used to measure chlorophyll. In this method, algal cells are isolated on a filter paper and MgCO_3 is used to restrict the degradation of chlorophyll during the measurement. Subsequently, the chlorophyll within the algae is released into 90% acetone by disrupting the cells using a sonicator. This process, called homogenization, is followed by an overnight extraction of the photosynthetic pigments at a temperature of 4°C. The solubilized pigments are then separated from residual matter by centrifugation at 5000 rpm for 10 minutes at 5°C. Spectrophotometric analysis of the resulting filtrate is used to obtain concentration of chlorophyll and its degradation products. Chlorophyll a and pheophytin a is estimated by measuring absorbance before and after acidification (Geider and Osborne, 1992).

The spectrophotometric equation used for estimating chlorophyll a and pheophytin a concentrations are as follows (APHA, 1999; Geider and Osborne, 1992);

$$[\text{chlorophyll a}] = 26.7 \times (E_{664} - E_{665}) \times (V_1/V_2/L) \quad \mu\text{g/L} \quad (2.3)$$

$$[\text{pheophytin a}] = 26.7 \times ((1.7 \times E_{665}) - E_{664}) \times (V_1/V_2/L) \quad \mu\text{g/L} \quad (2.4)$$

where,

E_{664} = (Optical density of filtrate at 664 nm) – (Optical density of filtrate at 750 nm)

E_{665} = (Optical density of acidified filtrate at 665 nm) – (Optical density of acidified filtrate at 750 nm)

V_1 = volume of 90% acetone used in extraction in millilitres

V_2 = volume of water filtered in litres

L = pathlength of cuvette used in centimetres

Yield of lipids. Algal lipids are highly valuable in the production of biodiesel. The lipid content of *C. vulgaris* was determined for one operating condition and compared with results obtained by Packer (2009). In this research, the Soxhlet extraction method was used to determine the lipid content. The Soxhlet extraction thimble was initially vacuum dried at 65°C and weighed after cooling to room temperature. Vacuum dried algal sample obtained from the circulating loop photobioreactor was then added to Soxhlet thimble and weighed once again. A dry receiving flask was prepared with several boiling chips. The flask was weighed with the boiling chips. Later, the Soxhlet apparatus was set up using 130 mL of pure ethyl ether. The boiling flask was inserted and heated at reflux for 12 hours. The reflux rate was adjusted such that four to five solvent exchanges were obtained in an hour. When the extraction was complete, the thimble was removed from the Soxhlet apparatus and the leftover sample was vacuum dried to remove any residual solvent. The solvent in the boiling flask was then evaporated using a rotary evaporator and vacuum oven. After evaporation, the flask was cooled to room temperature and weighed. Lipid content of the algal sample used was determined from the difference between the initial and final weight of the boiling flask.

2.3 RESULTS AND DISCUSSIONS

2.3.1 Yield of biomass

A typical batch growth cycle involves 5 phases; lag phase, exponential phase, deceleration phase, stationary phase and death phase (Shuler and Kargi, 2002). Figure 2.8 shows the growth pattern obtained in the circulating loop photobioreactor at a radiant flux of 26.945 mW. The pattern obtained reveals a short lag phase followed by exponential phase (between 10 to 288 hours) and the beginning of a stationary phase at the 288th hour. Since the non-substrate limited multiplication and growth of cells occur in the exponential phase, the net specific growth rate is determined from this phase. The biomass concentration for the exponential phase is given by;

$$\frac{dX}{dt} = (\mu_{\text{net}})X \quad (2.1)$$

where,

μ_{net} is the net specific growth rate.

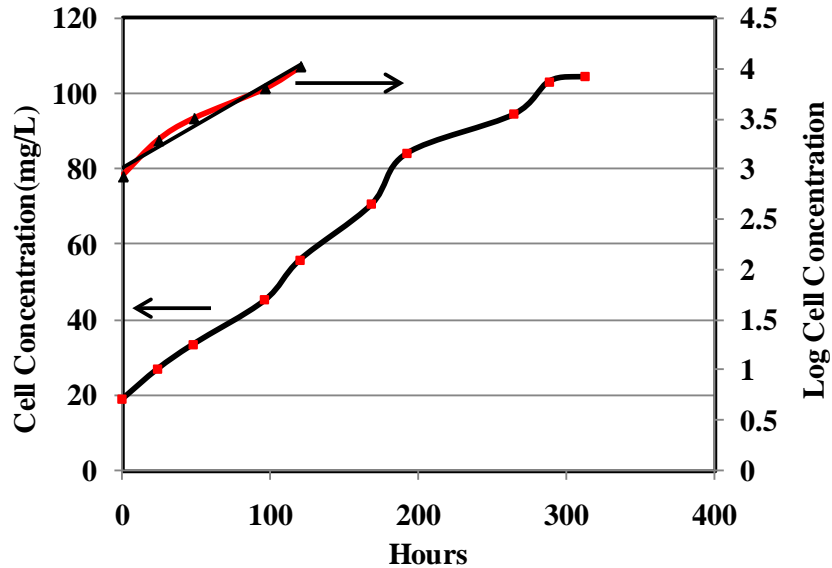


Figure 2.8 Transient changes in dry cell weight of *C. vulgaris* at radiant flux of 26.945 mW

C. vulgaris was found to consume CO₂ with a maximum biomass yield coefficient of 0.445 mg biomass/mg of CO₂. This value agrees reasonably well with the yield of 0.51 mg biomass/mg of CO₂ obtained by Powell *et al.* (2009a) and 0.52 mg biomass/mg of CO₂ determined by Javanmardian and Palsson (1992). Table 2.3 shows the biomass yield obtained, when no dark phase was provided, at different concentrations of CO₂. The data shows that at high CO₂ loadings, the biomass yield decreases suggesting that CO₂ may be inhibitory at higher concentrations.

On comparison of biomass yields obtained at the two conditions, it is evident that the dark phase plays a significant role in the growth of *C. vulgaris*. At similar conditions of CO₂ and concentration of nutrient medium, the yield of *C. vulgaris* showed an average percentage increase of 36.22% on providing a continuous 8 hour dark phase.

Table 2.3 Yield of biomass obtained at condition (i) with no additional dark phase

BULB	Total Volume (mL)	BOLD's Media (mL)	Air & CO₂ Mixture (mL)	Volume CO₂ (10% of Air Mix in mL)	Mass CO₂ (mg)	Initial Optical Density	Initial Dry Weight (mg_{DW}/L)	Final Optical Density (0%)	Final Dry Weight (mg_{DW}/L)	Yield of Biomass (mg_{DW}/mg CO₂)
1	136.5	34	102.4	10.7	21.1	0.051	10.70	0.556	138.00	0.205
2	135.6	68	67.4	7.0	13.9	0.029	5.40	0.337	82.80	0.378
3	137.4	102	35.0	3.7	7.3	0.019	3.40	0.148	35.20	0.445

Table 2.4 Yield of biomass obtained at condition (ii) with 8 hour dark phase

BULB	Total Volume (mL)	BOLD's Media (mL)	Air & CO₂ Mixture (mL)	Volume CO₂ (10% of Air Mix in mL)	Mass CO₂ (mg)	Initial Optical Density	Initial Dry Weight (mg_{DW}/L)	Final Optical Density (0% Dilution)	Final Dry Weight (mg_{DW}/L)	Yield of Biomass (mg_{DW}/mg CO₂)
1	136.50	34	102.4	10.2	20.3	0.072	16.03	0.74	184.30	0.283
2	135.60	68	67.4	6.7	13.3	0.040	7.96	0.45	111.81	0.532
3	137.40	102	35.0	3.5	6.9	0.028	4.94	0.18	44.01	0.577

2.3.2 Effect of light intensity on growth rate of *C. vulgaris*

The effect of light intensity on the growth rate of *C. vulgaris* is shown in Table 2.5. The growth rate of *C. vulgaris* was studied at an optimum CO₂ concentration of 10% (v/v) as suggested by Powell *et al.* (2009a). By varying the radiant flux from 26.945 mW to 431.128 mW the specific growth rate could be increased by a factor of 3.6. Hence, it can be concluded that radiant flux incident on the surface of the photobioreactor has a direct relationship with the growth rate of *C. vulgaris* (shown in Figure 2.9). This shows that the intensity of light is a major parameter controlling the growth of *C. vulgaris*. The highest growth rate for *C. vulgaris* reported by Muranaka and Murakami (2001) under high light conditions was close to 0.03 h⁻¹. This value is comparable with the results obtained in this study.

In this study, a maximum specific growth rate of 0.029 h⁻¹ could be obtained for *C. vulgaris* for the highest value of radiant flux of light used at 10% (v/v) of CO₂. It could be speculated that higher light intensity would further increase specific growth rate. However, this phenomenon could not be studied since additional lights could not be fixed to the photobioreactor surface.

Table 2.5 Effect of various parameters on the growth rates of *Chlorella vulgaris* at 10% (v/v) of CO₂

Run	Lights	Radiant flux (mW)	Radiant Flux Density (W/m ²)	CO ₂ Flowrate (ml/min)	Air Flowrate (ml/min)	Chlorophyll	μ (day ⁻¹)	μ (h ⁻¹)
1	1	26.945	0.075	20	180	2.50%	0.200	0.0080
2	2	53.891	0.149	20	180	NA	0.243	0.0101
3	4	107.782	0.298	20	180	2.45%	0.278	0.0116
4	6	161.673	0.448	20	180	2.00%	0.520	0.0220
5	10	269.455	0.747	20	180	0.13%	0.632	0.0260
6	16	431.128	1.195	20	180	0.86%	0.700	0.0290

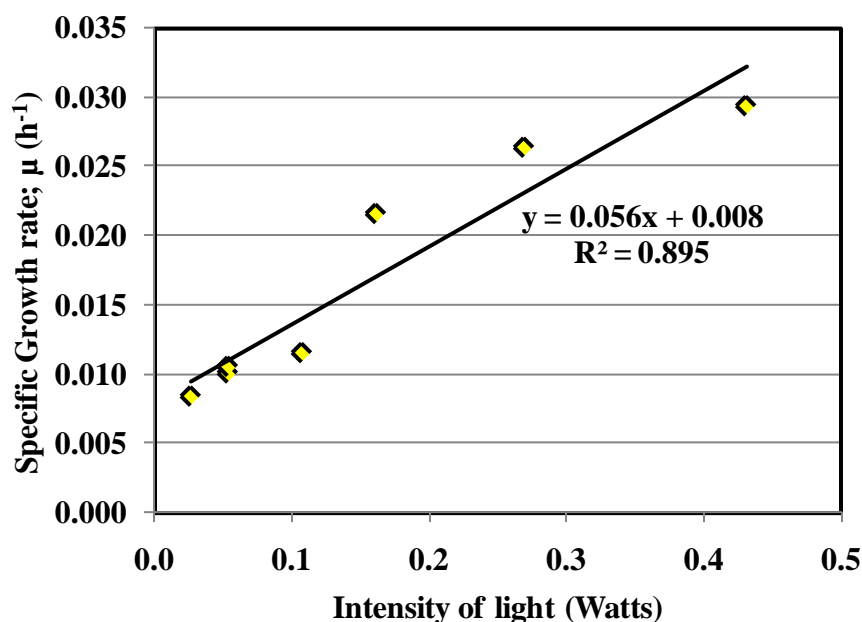


Figure 2.9 Variation of specific growth rate with intensity of light incident on the surface of photobioreactor. Operating conditions: 10% (v/v) CO_2 ; short intervals of light and dark phase

2.3.3 Effect of light – dark cycle on growth rate of *C. vulgaris*

Often researchers have studied the effects of excess light or photoinhibition on the growth of microalgal species (Adir *et al.*, 2003; Suh and Lee, 2001). However, the effect of a dark phase on specific growth rate has not often been considered. Table 2.6 shows the effect that an additional 8 hour continuous dark phase has on the growth rate of *C. vulgaris*. Keeping the radiant flux constant and implementing a continuous dark phase resulted in boosting the growth rate at all conditions examined. The highest increase was at a radiant flux of 161.673 mW where the growth rate increased by a factor of 1.73 on addition of a continuous dark phase.

Table 2.6 Effect of continuous 8 hour dark phase on the specific growth rate of *C. vulgaris* at 10% (v/v) of CO₂ concentration

Run	Radiant flux (mW)	Radiant flux density (W/m ²)	Additional dark phase	Chlorophyll	μ (day ⁻¹)	μ (h ⁻¹)
1	161.673	0.448	No	2.00%	0.518	0.0216
2	161.673	0.448	Yes	3.83%	0.897	0.0374
3	215.564	0.597	Yes	3.65%	0.895	0.0373
4	269.455	0.747	No	0.13%	0.632	0.0263
5	269.455	0.747	Yes	4.24%	0.821	0.0342
6	431.128	1.195	No	0.86%	0.703	0.0293
7	431.128	1.195	Yes	1.62%	0.728	0.0303

2.3.4 Effect of CO₂ concentration on growth rate of *C. vulgaris*

Since incorporating a continuous 8 hour dark phase proved successful in increasing growth rates of *C. vulgaris*, CO₂ concentration effects were conducted in the presence of the continuous dark phase. Table 2.7 shows the variation in specific growth rate of *C. vulgaris* due to change in the concentration of CO₂ flowing into the reactor. The value of radiant flux was kept constant to study the effect of CO₂. It was observed that the growth rate has an inverse relation with the concentration of CO₂. Hill (2006) showed that a 5% (v/v) concentration of CO₂ results in a dissolved CO₂ concentration 1.7x10⁻³ M (72 mg/L). Similarly, 10% (v/v) and 15% (v/v) CO₂ would result in dissolved CO₂ concentration of 3.5x10⁻³ M (150 mg/L) and 5x10⁻³ M (214 mg/L). An increase in the dissolved CO₂ concentration from 72 mg/L to 214 mg/L resulted in a decrease in the growth rate by a factor of 3.3. The highest growth rate of 0.043 h⁻¹ obtained in this research for *C. vulgaris* was at a CO₂ concentration of 5% (v/v), radiant flux of 161.673 mW and in the presence of a continuous 8-hour dark phase. This value is the highest growth rate that has been measured for the *C. vulgaris*. Myers and Killam (1956) obtained a growth rate of 0.023 h⁻¹ with 4% CO₂ and saturating light provided by banks of daylight fluorescent lamps. Enhanced growth rates in the novel circulating loop photobioreactor could be attributed to the appropriate

combination of the right amount of CO₂ and light. Even higher rates may likely be achieved if other combinations were attempted, such as higher intensities of light at 5% (v/v) CO₂.

Table 2.7 Effect of CO₂ concentration on the specific growth rate of *C. vulgaris*

Run	Lights	Radiant flux density (W/m ²)	Radiant Flux of light (mW)	CO ₂ Flowrate (ml/min)	Volumetric concentration of CO ₂	Air Flowrate (ml/min)	Chlorophyll	μ (day ⁻¹)	μ (h ⁻¹)
1	6	0.448	161.673	0	0%	200	3.78%	0.360	0.0150
2				10	5%	190	4.52%	1.032	0.0430
3				20	10%	180	3.83%	0.897	0.0374
4				30	15%	170	1.05%	0.312	0.0130

A study of the CO₂ evolved from the gas-liquid separator region of the reactor can give an idea of the amount of CO₂ utilized by the algal cells for photosynthesis. Figure 2.10 shows the decrease in concentration of CO₂ evolved from the reactor as the cell concentration of the algal cells increases. This pattern observed shows that as the cell concentration increases, the consumption of CO₂ increases and subsequently the concentration of CO₂ evolved from the bioreactor decreases. At a low cell concentration of 7.204 mg/L the CO₂ evolved from the bioreactor was found to be 0.8320 V. As the cell concentration increased to a value of 217.176 mg/L, CO₂ evolved from the bioreactor reduced to 0.4396 V. It was also observed that during the 8 hour dark phase, the concentration of CO₂ evolved from the bioreactor increases since photosynthesis is stopped. In Figure 2.10, point 1 to point 2 shows the change in CO₂ evolved from the bioreactor during the light phase. As the light phase proceeds from point 1 (hour 118.34) to point 2 (hour 133.9), the CO₂ evolved decreases from 0.5976 V to 0.4817 V. At point 2, the dark phase of reactions begins. CO₂ evolved from the bioreactor increases from a value of 0.4817 V at the beginning of dark phase to 0.5607 V at the end of dark phase. On an average, a 15% to 16% decrease in evolution of CO₂ from the bioreactor was observed during the dark phase.

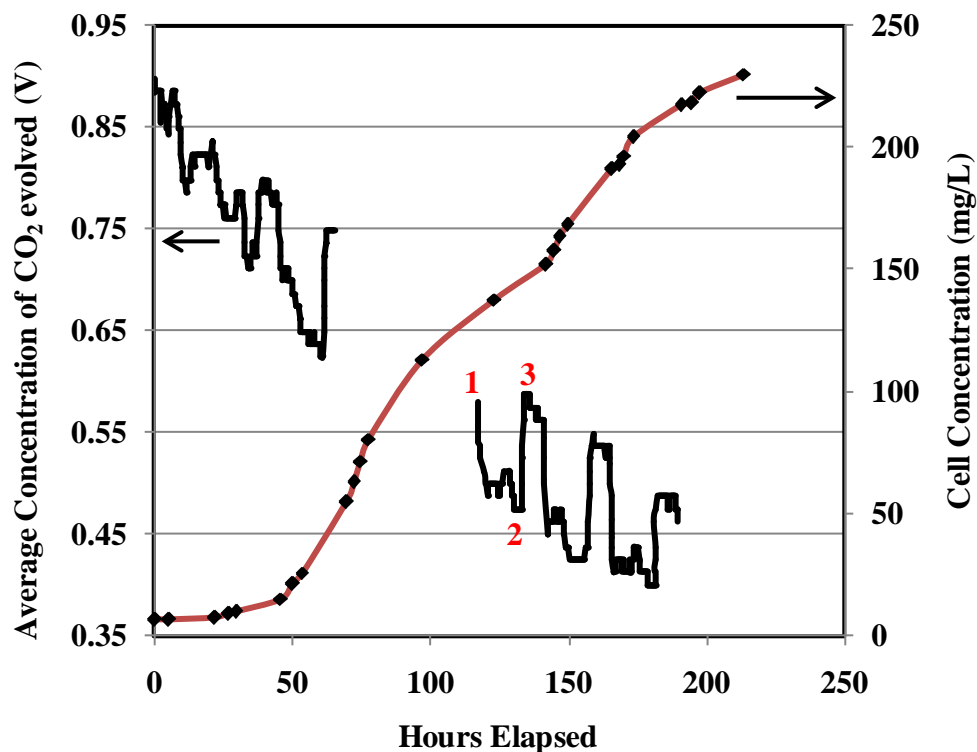


Figure 2.10 Variation in concentration of CO₂ evolved from reactor as the concentration of cells in the reactor volume increase. Region from point 1 to point 2 indicates the CO₂ evolved during light phase while the region from point 2 to point 3 shows CO₂ evolved during dark phase. This study was conducted at 5% (v/v) concentration of CO₂ and 161.673 mW radiant flux of light.

2.3.5 Yield of Chlorophyll and Lipids

In microalgae, the ratio of chlorophyll to biomass has been reported to range from 0.1% to 5% of dry weight (Geider and Osborne, 1992). The concentration of chlorophyll varies with the cell concentration. Variation of chlorophyll concentration follows the same pattern as the growth of cells (Young *et al.*, 1996). Hence, the highest concentration of chlorophyll will be obtained at the highest cell concentration or at the end of the exponential phase of growth. Chlorophyll concentrations were determined for the various conditions of CO₂ concentration, radiant flux and presence of additional dark phase. The higher concentration of 4.52% as shown in Table 2.7 was obtained towards the conclusion of the exponential phase.

Algal lipids are valuable products that can be used for the production of biodiesel. *Chlorella vulgaris* is known to have a lipid content of 14 - 22% which is mainly composed of poly unsaturated fatty acids (Tokusoglu and Unal, 2003; Packer, 2009). Studies conducted with algal biomass produced in the circulating loop photobioreactor were found to have a lipid concentration of 6.79% to 12.50% by weight of algal cells. Interestingly, the intensity of light and CO₂ concentration available in the photobioreactor seemed to have an effect on the lipid concentration of *C. vulgaris*. At the optimum value of light intensity at 161.673 mW and CO₂ concentration of 5% (v/v), a higher biolipid concentration of 12.5% was obtained.

Table 2.8 Lipid concentration of *C. vulgaris*

Run	Lights	Intensity of light (mW)	CO ₂ Flowrate (ml/min)	Volumetric concentration of CO ₂	Air Flowrate (ml/min)	μ (h ⁻¹)	Lipids
2	10	269.455	30	15%	170	0.015	6.79%
1	6	161.673	10	5%	190	0.043	12.50%

2.4 REPRODUCIBILITY

The reproducibility of the studies was determined. Duplicate runs were performed for three conditions as shown in Table 2.9. On average, the percent change in the measured specific growth rate was 4.84%.

Table 2.9 Reproducibility of growth rate data from the circulating loop photobioreactor

Run	Lights	Radiant flux density (W/m ²)	Radiant flux (mW)	CO ₂ Flowrate (ml/min)	Air Flowrate (ml/min)	Chlorophyll	μ (day ⁻¹)	μ (h ⁻¹)
with short intervals of light and dark phase and 10% (v/v) CO₂								
1	2	0.149	53.891	20	180	NA	0.243	0.0101
rerun	2	0.149	53.891	20	180	3.55%	0.256	0.0106
with 8 hour dark phase and 10% (v/v) CO₂								
1	10	0.747	269.455	20	180	1.88%	0.700	0.0326
rerun	10	0.747	269.455	20	180	4.24%	0.821	0.0342
with 8 hour dark phase and 5%(v/v) CO₂								
1	6	0.448	161.673	10	190	4.52%	1.0320	0.0430
rerun	6	0.448	161.673	10	190	2.74%	0.984	0.0410

3.0 EFFECT OF LIGHT INTENSITY AND CO₂ ON GROWTH OF *Chlorella vulgaris* IN A CONTINUOUS FLOW MIXED PHOTOBIOREACTOR

3.1 INTRODUCTION

A continuous flow mixed bioreactor is an essential tool in physiological studies. Analyses carried out in a continuous reactor can provide valuable information on the metabolism of microorganisms (Nielsen *et al.*, 2003). A steady-state microbial population consists of cells of all possible sizes and developmental stages. Hence, the observed growth rate of such steady-state algal suspensions is actually a statistical average of characteristics of individual cells (Schuler and Kargi, 2002). Continuous mode photobioreactors are valuable in studying effects of multiple parameters on an output variable. As such, in this research, an externally illuminated continuous flow mixed photobioreactor was used to study the interactive effects of light intensity, dilution rate and CO₂ concentration on the specific growth rate of *C. vulgaris*. The continuous flow stirred bioreactor was used as it is a closed system that allows for minimum contamination of the culture in the reactor and easy control of culture parameters such as pH, oxygen, carbon dioxide concentration, and temperature (Barsanti and Gualtieri, 2006).

The main objective of this part of the research project was to study the interacting effects of light intensity at varying concentrations of carbon dioxide and flowrate of nutrient medium in a continuous flow mixed reactor on the specific growth rate of *C. vulgaris*.

3.2 EXPERIMENTAL SETUP AND PROCEDURES

3.2.1 Cells and media

Chlorella vulgaris culture was obtained from Carolina Biological Supply (Burlington, North Carolina, catalogue No. 15-2075). The algae were grown in modified Bolds basic media. The composition of the nutrients was 7.5 mg KH₂PO₄, 50 mg K₂HPO₄, 75 mg NH₄Cl, 25 mg MgSO₄·7H₂O, 12.5 mg CaCl₂, 12.5 mg NaCl, 60 mg NaHCO₃, 25 mg EDTA (sodium salt), 2.5

mg $\text{FeSO}_4 \cdot 7\text{H}_2\text{O}$ and 0.5 mL of trace mineral solution (1250 mg boric acid, 882 mg ZnSO_4 , 71 mg MoO_3 , 49 mg $\text{Co}(\text{NO}_3)_2$, 144 mg MnCl_2 , 157 mg $\text{CuSO}_4 \cdot 7\text{H}_2\text{O}$ in 100 millilitres of reverse osmosis water) per litre of media (Powell *et al.*, 2009a). The pH of the media was adjusted to 6.8 which is within the optimum pH range (as mentioned on page 6) for growth of *C. vulgaris* cells. Freshly prepared media was sterilized in an autoclave at 120°C for 15 minutes and later cooled to room temperature prior to use in the reactors.

3.2.2 Experimental Setup

The continuously mixed photobioreactor is shown in Figure 3.1. The photobioreactor used was a BIOFLO Model C-30 manufactured by New Brunswick Scientific Co. The BIOFLO allows advanced control of the culture environment which enables accurate study of growth rate of microorganisms. This particular model has often been used for biokinetic study of organisms. The reactor vessel, used in this research, is constructed of Pyrex glass and has a liquid capacity of 1475 mL. Airflow into the bioreactor was supplied via a flowmeter through a large holed sparger. Although, earlier studies (Powell *et al.*, 2009a; Yanagi *et al.*, 1995) showed that *Chlorella* sp. has optimum growth at 10% CO_2 , in this research 0%, 5%, 10% and 15% (v/v) concentrations of CO_2 were studied. All concentrations of CO_2 mentioned should be added to the atmospheric concentration of CO_2 (0.03%). To maintain a continuous mode, fresh sterile Bold's media was pumped into the continuously stirred bioreactor at a steady flow rate and cell suspension from the bioreactor was removed constantly to maintain constant liquid volume. The effects of high and low flowrates of media were studied. The high media flowrate used in this study was 14 mL/hr and the lower flowrate was 7 mL/hr. The photobioreactor was externally illuminated using a compact fluorescent bulb as shown in Figure 3.2. The interacting effects of light intensity and CO_2 concentration were studied at two light levels; radiant flux of 119.2 mW and 93.4 mW. Variation of light intensity was facilitated by modifying the distance between the surface of bioreactor and the light source. Figure 3.3 depicts the variation in radiant flux incident on the surface of the bioreactor with distance from the bioreactor. While the higher intensity was obtained by placing the light source at a distance of 10 centimetres from the reactor, lower light intensity was obtained at a distance of 40 centimetres. The light radiation from the fluorescent bulb was found to have the spectral irradiance as shown in Figure 3.4. The spectrum of the

fluorescent bulb matches the absorption spectra of *C. vulgaris* (as mentioned on page 6). However, the irradiance in the region 660 – 700 nm is low.

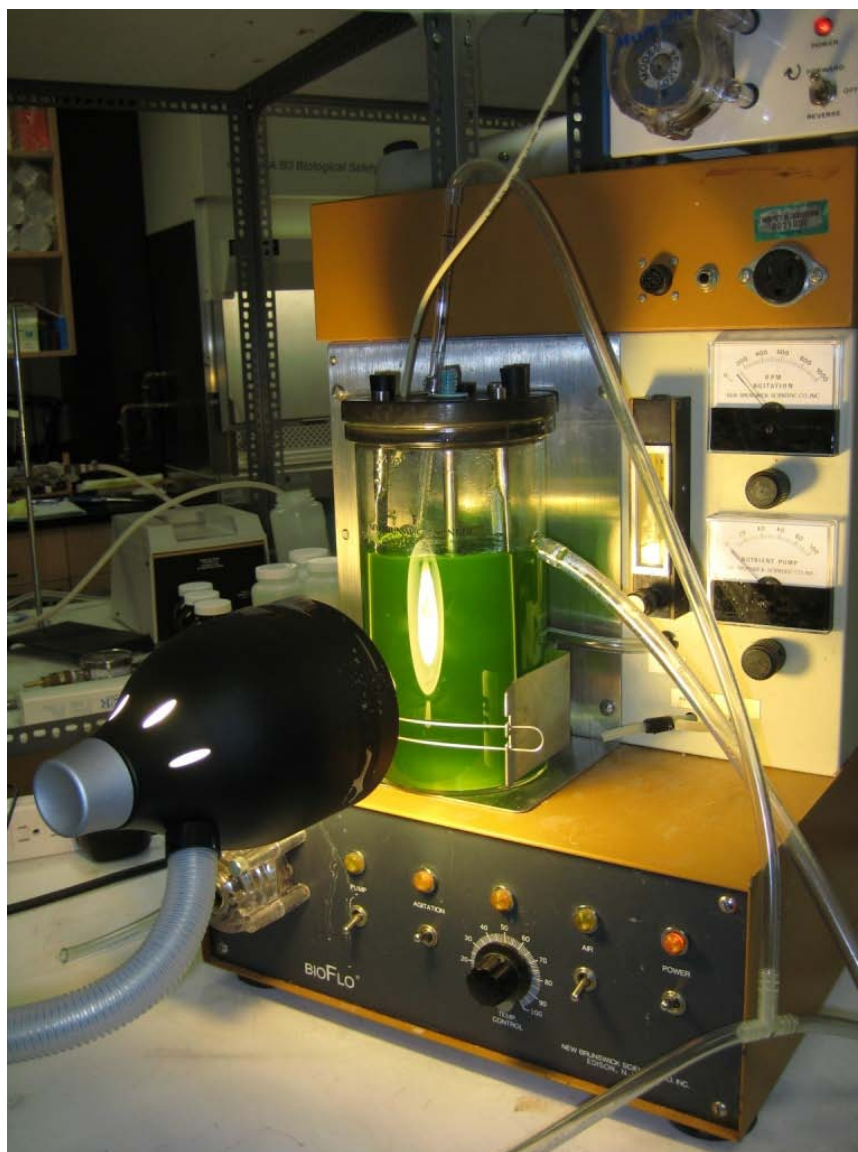


Figure 3.1 Continuously mixed photobioreactor containing the photosynthetic algae *C. vulgaris*.

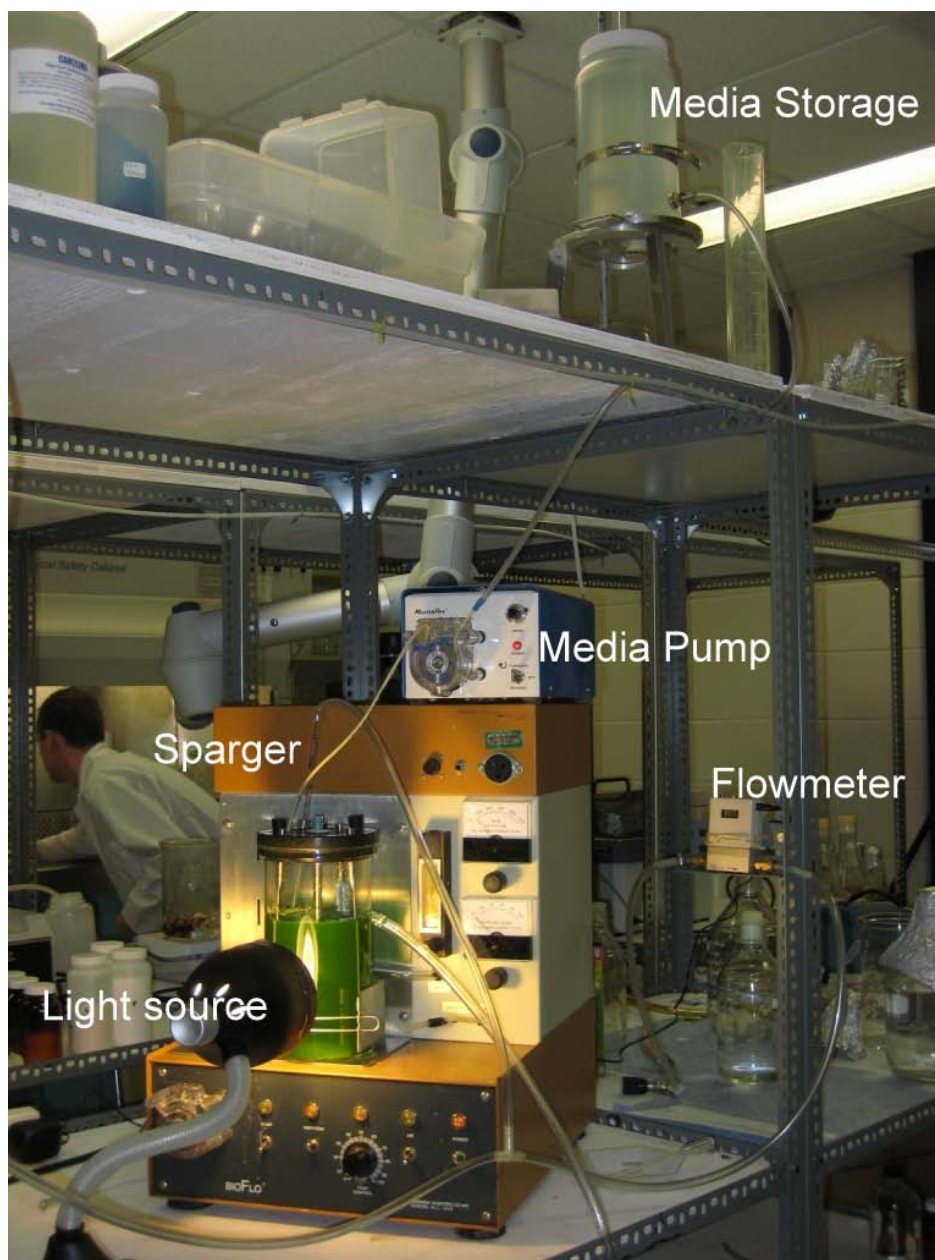


Figure 3.2 Complete experimental set-up showing the continuously mixed photobioreactor with a fluorescent light source, sparger, pump for media flow and flow meter to measure airflow.

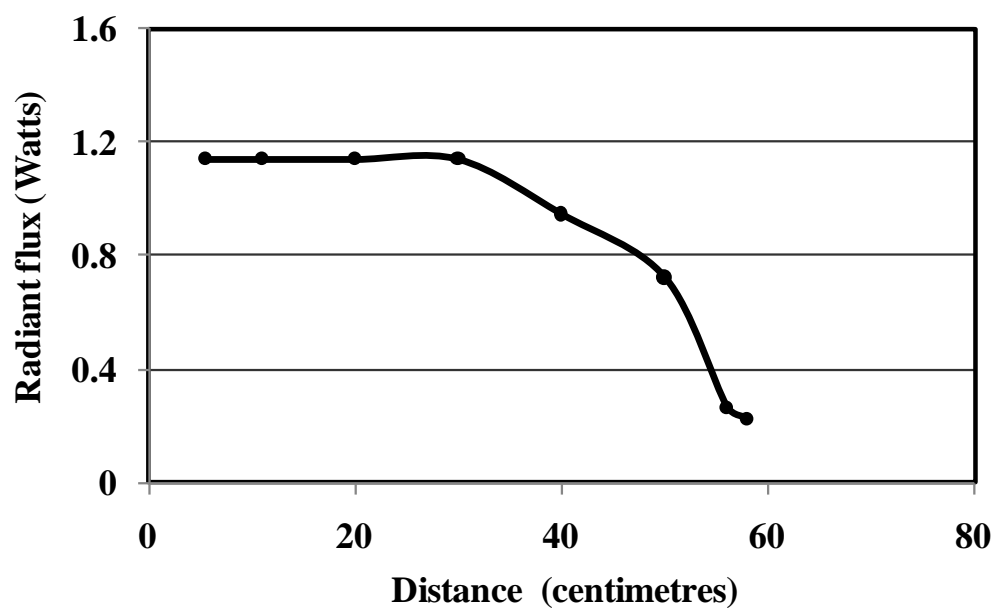


Figure 3.3 Variation in radiant flux incident on the surface of the bioreactor with distance from the bioreactor.

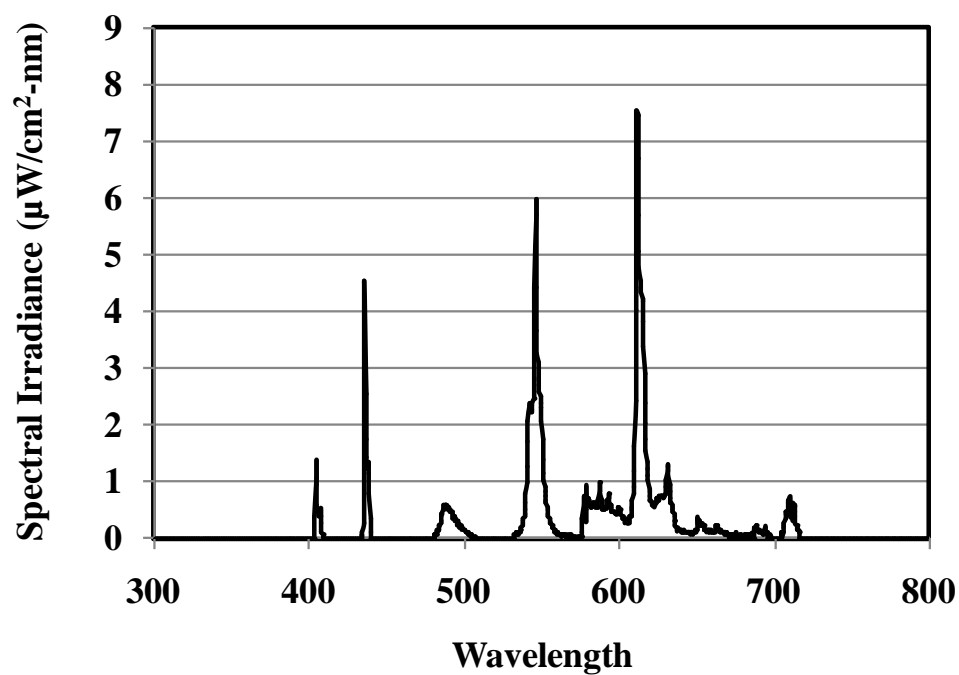


Figure 3.4 Scan of light irradiance from the fluorescent bulb.

3.2.3 Analytical Methods Used

Measurement of biomass. Biomass concentration of the medium is determined based on the optical density. In order to determine the optical density, a Shimadzu model 1240 spectrophotometer (Shimadzu Corporation, Kyoto, Japan) was used at a wavelength of 620 nm. Reverse osmosis water was used as reference. Daily samples were analysed spectrophotometrically from the reactor.

The dry weights of samples of *C. vulgaris* biomass were measured as a function of the absorbance at 620 nm in the Shimadzu spectrophotometer. Figure 3.5 shows the dry weight calibration curve that was obtained. The relationship between the dry weight and absorbance was determined as;

$$X = 246.25 \times OD_{620} \quad (3.1)$$

where,

X = biomass concentration in mg dry weight per litre

OD₆₂₀= optical density of sample measured at 620 nm

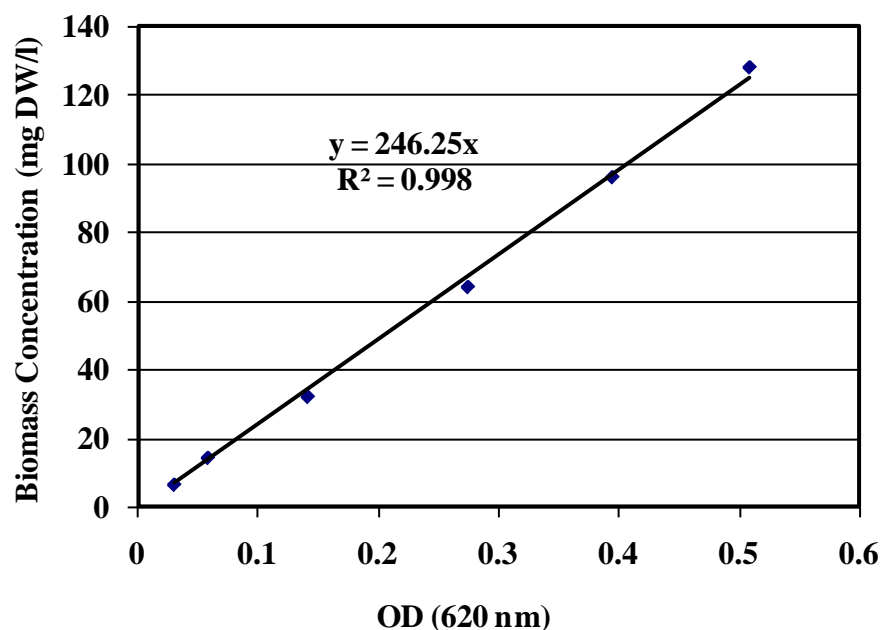


Figure 3.5 Dry weight calibration curve for Shimadzu model 1240 spectrophotometer at 620 nm.

Determination of cell density using Petrov-Hauser counter. A reliable and traditional method of quantifying algal cells is counting. Counting of microalgal cells is done under a microscope using a counting chamber. This procedure allows for direct examination and evaluation of the algal cells. A number of counting chambers such as the Sedgewick-Rafter, Thoma and Petrov-Hauser are used commonly in counting and taxonomic identification (Barsanti and Gualtieri, 2006). Each of these counting chambers has a grid etched upon the surface. The dimension of this grid is essential to determine the number of cells per millilitre of the algal sample used. Figure 3.6 shows the dimensions of the grid on Petrov-Hauser counting chamber used in this research. Approximately 0.1 ml of the microalgal sample is placed on the counting chamber and covered with a cover slip. The chamber is then viewed under a 150x Bausch and Lomb inverted microscope. Figure 3.7 shows a microscopical view of *C. vulgaris* cells on a Petrov-Hauser counter. The number of cells in each square of the grid is counted. This value is then used to obtain the number of cells per millilitre of sample as per the equation:

$$\text{Number of Cells / mL} = \frac{C}{V \times F} \quad (3.2)$$

where,

C = the number of cells counted

V = volume of each square on the Petrov-Hauser counter

$$= (50 \times 50 \times 20) \mu\text{m}^3 = 5 \times 10^{-8} \text{ ml}$$

F = number of squares counted

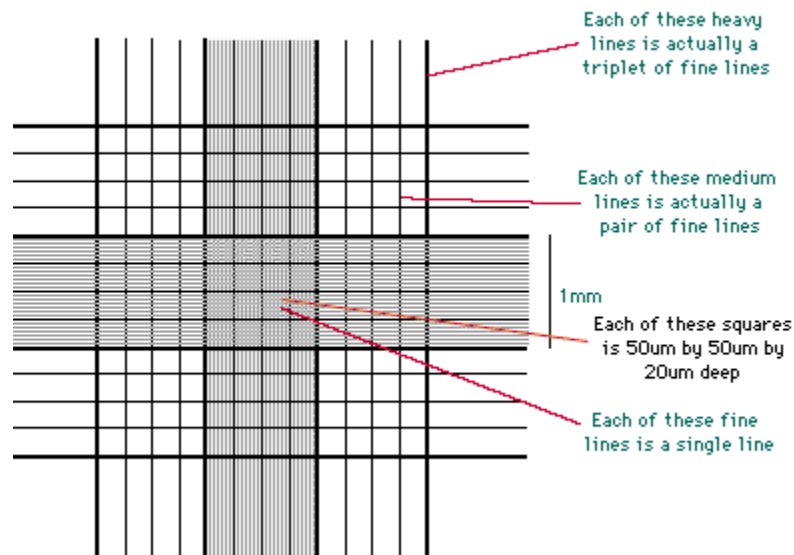


Figure 3.6 Schematic drawing of the grid on a Petrov-Hauser counting chamber (Brown, 2009). Each of the squares on the counter is 50 μm by 50 μm by 20 μm deep.

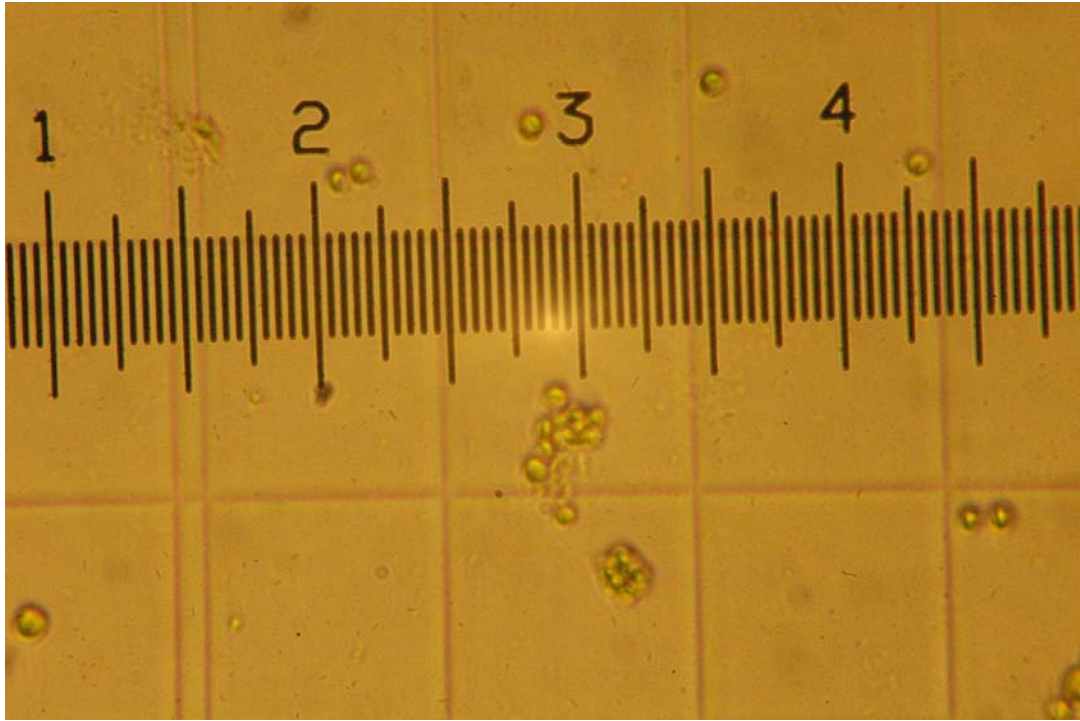


Figure 3.7 Microscopic view of *C. vulgaris* cells on a Petrov-Hauser counting chamber. A stage micrometer having a scale of 1 division = 5.14 μm was used in the microscope and is shown in the figure.

3.3 RESULTS AND DISCUSSIONS

3.3.1 Yield of biomass

In a continuously stirred reactor that is fed with sterile growth medium, containing a growth rate limiting substrate, at steady state the specific growth rate is equivalent to the dilution rate (Shuler and Kargi, 2002) ;

$$\mu = D, \quad (3.5)$$

where,

μ is the specific growth rate (h^{-1})

D is the dilution rate and reciprocal of residence time, (h^{-1}).

The Monod equation (Goldman *et al.*, 1974):

$$\mu = \frac{\mu_m S}{(K_s + S)} \quad (3.6)$$

where,

μ_m is the maximum specific growth rate (h^{-1})

S is the concentration of the limiting nutrient (mg/L)

K_s is the half-saturation coefficient (mg/L)

implies that the growth rate will be limited by the growth substrate. But in case of this study, it is observed that the substrate concentration remains independent of the dilution rate. This is because the growth substrate (CO_2) is supplied instantaneously through the sparger. Therefore the cells are constantly growing at a maximum growth rate and will never achieve steady state. Figure 3.8 illustrates this phenomenon. The biomass concentration for this case can be predicted from:

$$\frac{dX}{dt} = (\mu_m - D)X \quad (3.7)$$

where X is the biomass concentration (mg / L)

The oscillatory pattern observed at low dilution rates such as shown in Figure 3.9 was also observed by Javanmardian and Palsson (1992). At similar interacting conditions of CO_2 concentration, low dilution rate of nutrient medium and high intensity of light, Javanmardian and Palsson showed that the accumulation of inhibitory chemicals in the bioreactor can hinder the achievement of steady state and cause the cell concentration to fluctuate in an oscillatory fashion.

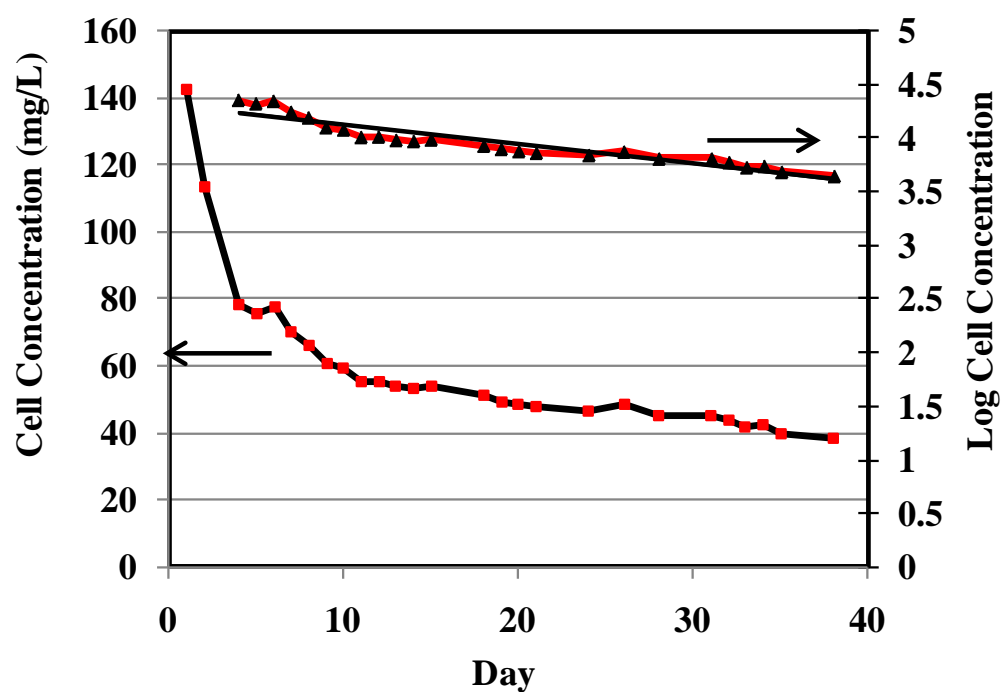


Figure 3.8 Transient changes in dry cell weight of *C. vulgaris* at a dilution rate of 0.01 h^{-1} , 5% (v/v) CO_2 concentration and 93.415 mW radiant flux

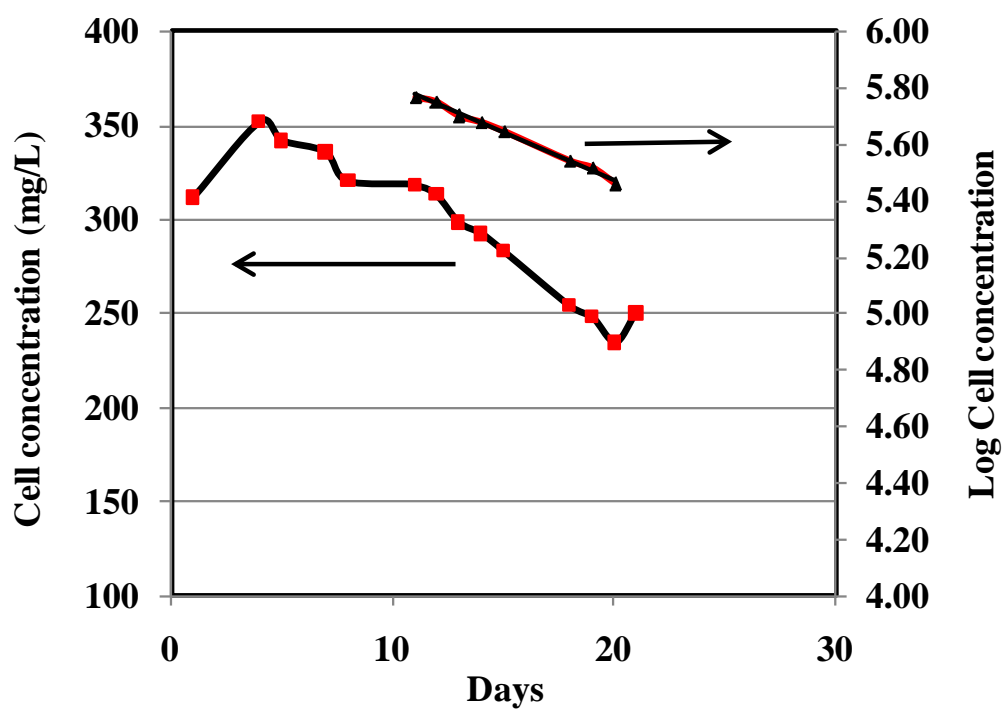


Figure 3.9 Transient changes in dry cell weight of *C. vulgaris* at dilution rate of 0.005 h^{-1} , 15% (v/v) CO_2 and 119.225 mW radiant flux

3.3.2 Effect of dilution rate, concentration of CO₂ and light intensity on growth rate

The effect of the dilution rate and concentration of carbon dioxide on the maximum growth rate of *C. vulgaris* is shown in Table 3.1. The dilution rate has an effect on the specific growth rate of *C. vulgaris*. The higher dilution rate in general improved the growth rate, likely due to lesser accumulation of inhibitory by-products than at low dilution rates as reported by Javanmardian and Palsson (1992). The interacting effect of high intensity light and high dilution rate proved to result in the highest growth rates at higher CO₂ concentrations of 10% (v/v) and 15% (v/v). For instance, at 10% (v/v) CO₂ concentration, a high dilution rate combined with high intensity light increased the growth rate of *C. vulgaris* by a factor of 1.8 when compared to the growth rate obtained at similar CO₂ concentration and dilution rate but a lower intensity of light.

From the data obtained, the average growth rate for low intensity light is 0.00696 h⁻¹ and the average growth rate at high intensity of light is 0.00732 h⁻¹. This 5% improvement in growth rate shows that the intensity of light is also a major parameter controlling the growth of *C. vulgaris*. Studies by Powell *et al.* (2009a) showed that at a radiant flux of 32.3 mW, a concentration of 5% (v/v) CO₂ was less efficient than the 10% (v/v) CO₂. In this study, high growth rates of 0.00929 h⁻¹ were obtained at a CO₂ concentration of 5% (v/v) and dilution rate of 0.01 h⁻¹ and radiant flux of 93.415 mW. This value was close to the highest growth rate (0.00979 h⁻¹) obtained at 10% (v/v) CO₂, dilution rate of 0.01 h⁻¹ and 119.225 mW radiant flux.

Microorganisms like algae react to environmental stresses by production of inhibitory substances or alteration of metabolic pathways (Javanmardian and Palsson, 1991, Axelsson and Beer, 2001). At higher light intensities, the carbon utilization mechanisms of most algae may be altered (Axelsson and Beer, 2001). It may be considered that when light stress is combined with the stress of high CO₂ concentration a decrease in growth rate of the algae occurs due to production of inhibitory products. In the circulating loop photobioreactor operated in fed-batch mode, a similar decrease in growth rate was observed on increasing the CO₂ concentration from 5% (v/v) to 15% (v/v). When inhibitory substances are produced, high dilution rates would prevent the accumulation of these compounds and can effectively enhance growth rates. This

pattern can be seen by observing the growth rates of 15% (v/v) CO₂ at high light intensity. The dilution rate was increased from 0.005 h⁻¹ to 0.01 h⁻¹ while maintaining the CO₂ concentration at 15% (v/v) and radiant flux at 119.225 mW. The growth rate increased from 0.00404 h⁻¹ at low dilution rate to 0.00871 h⁻¹ at high dilution rate. An increase in the dilution rate enabled doubling the growth rate obtained at low dilution rate. Hence, the interacting effect of CO₂ concentration, dilution rate and intensity of light determines the maximum growth rate.

Table 3.1 Effect of various parameters on the growth rates of *C. vulgaris*

Run	CO ₂		Air (ml/min)	Media Flowrate (ml/hr)	Dilution Rate (h ⁻¹)	Light	Radiant Flux (mW)	Radiant Flux Density (mW/cm ²)	Slope of lnX v/s time graph (hr ⁻¹)	μ_m (hr ⁻¹) Specific growth rate
	ml/min	% volumetric concentration								
1	0	0%	200	7	0.005	High	119.2	0.127	-0.00700	-0.00029
2	10	5%	190	14	0.010	High	119.2	0.127	-0.00646	0.00350
3	10	5%	190	14	0.010	Low	93.4	0.0994	-0.000750	0.00925
4	10	5%	190	7	0.005	Low	93.4	0.0994	0.00122	0.00622
5	20	10%	180	7	0.005	High	119.2	0.127	0.00174	0.00674
7	20	10%	180	14	0.010	High	119.2	0.127	-0.000208	0.00979
6	20	10%	180	14	0.010	Low	93.4	0.0994	-0.00460	0.00540
8	30	15%	170	7	0.005	High	119.2	0.127	-0.000960	0.00404
9	30	15%	170	14	0.010	High	119.2	0.127	-0.00129	0.00871

3.4 REPRODUCIBILITY

The reproducibility of the conducted studies was determined. Duplicate runs were performed for the condition of 10% CO₂ concentration interacting with a dilution rate of 0.01 h⁻¹ and a radiant flux of 119.225 mW. The results obtained are shown in Table 3.2. A 1.69% change in the measured value of specific growth rate was observed in the duplicate run compared to the original run.

Table 3.2 Reproducibility of growth rate data obtained from the continuously stirred photobioreactor

Run	CO ₂		Air (ml/min)	Media Flowrate (ml/hr)	Dilution Rate (h ⁻¹)	Light	Radiant Flux (mW)	Radiant Flux Density (mW/cm ²)	Slope of lnX v/s time graph (hr ⁻¹)	μ_m (hr ⁻¹) Specific growth rate
	ml/min	% volumetric concentration								
1	20	10%	180	14	0.01	High	119.2	0.127	-0.000208	0.00979
rerun	20	10%	180	14	0.01	High	119.2	0.127	-0.000374	0.00963

4.0 CONCLUSIONS AND RECOMMENDATIONS

4.1. CONCLUSIONS

4.1.1. Novel Circulating Loop Photobioreactor

- Biomass yields determined for *C. vulgaris* produced comparable results to Powell *et al* (2009a) and Javanmardian and Palsson (1992). In our study, when biomass yield was determined from algal samples that were subjected to a radiant flux of 119.2 mW, studies revealed that 2.25 mg of CO₂ was required to produce 1 mg of biomass. But when studies were conducted with algal samples subjected to the same radiant flux with an 8 hour dark phase, only 1.73 mg of CO₂ was required to produce 1 mg of biomass. This is an important study to impose the significance of the dark phase in the growth of photosynthetic microorganisms.
- Studies conducted demonstrated for the first time, from known literature, holding all other growth parameters constant, the specific growth rate of *Chlorella vulgaris* increased as the light intensity incident on the surface of the photobioreactor increased. Hence, the efficient radiation of a circulating loop photobioreactor can significantly enhance growth rates of *C. vulgaris*. An increase in radiant flux from 26.9 mW to 161.6 mW resulted in a 175% increase in growth rate. But a further increase of radiant flux from 161.7 mW to 431.1 mW generated a smaller increase of 31% in growth rate of *C. vulgaris*. As such, it was concluded that a radiant flux of 161.7 mW is best for growth rate of *C. vulgaris*.
- Including a continuous 8 hour dark phase to the regular functioning of the circulating loop photobioreactor presented good results. The additional 8 hour dark phase significantly increased growth rate of *C. vulgaris* from 0.022 h⁻¹ to 0.0374 h⁻¹ at 10% (v/v) CO₂ and radiant flux of 161.7 mW. Therefore, the importance of a continuous 8 hour dark phase to enhance the growth rate of *C. vulgaris* has been demonstrated.

- Interesting results were obtained on changing volumetric concentration of CO₂ flowing into the reactor. While a 0% (v/v) concentration of CO₂ produced a low growth rate of 0.015 h⁻¹, increasing the concentration to 5% (v/v) resulted in the highest growth rate of 0.043 h⁻¹. A further increase in CO₂ concentration could not generate a corresponding increase in growth rate. Hence, it can be concluded that the best concentration of CO₂ for the growth rate of *C. vulgaris* is 5% (v/v) at a radiant flux of 161.7 mW.
- The nutrient value of *C. vulgaris* could be determined from the chlorophyll yield and lipid content. Since, chlorophyll content changes depending on the growth phase of the culture, these values could not be compared with any previous studies. Lipid content determined in this study was comparable to that obtained by Packer (2009). An interesting phenomenon observed was the increase in biolipid concentration at the optimum conditions of light intensity and CO₂ concentration. However, this phenomenon was not studied extensively as lipid extraction was not the main focus of this research.

The above points illustrate that the use of a novel circulating loop photobioreactor, that can precisely control light intensity, CO₂ concentration and dark phase duration, can successfully increase the growth rate and consequently increase carbon dioxide fixation rate of the *C. vulgaris* cells.

4.1.2. Continuous Flow Mixed Photobioreactor

- At the optimum concentration of 10% (v/v) CO₂, radiant flux of 119.2 mW and high dilution rate, the highest growth rate of 0.00979 h⁻¹ was obtained. The interacting effect of light intensity and concentration of CO₂ was studied extensively in the continuously stirred photobioreactor. At a dilution rate of 0.005 h⁻¹ and light intensity of 119.2 mW, an increase in CO₂ concentration from 10% (v/v) to 15% (v/v) resulted in a 40% decrease in growth rate of *C. vulgaris*. However, at a higher dilution rate of 0.01 h⁻¹ and light intensity of 119.2 mW, increasing the CO₂ concentration from 10% (v/v) to 15% (v/v) resulted in only an 11% decrease in growth rate. This considerable reduction in the

decrease of growth rate could be due to higher removal rate of inhibitory products at higher dilution rate. Hence, a higher dilution rate can counteract deleterious effects of stress due to high light intensity and high CO₂ concentrations.

- Similar to the fed-batch reactor, a high growth rate was obtained at a CO₂ concentration of 5% (v/v). At the CO₂ concentration of 5% (v/v), low radiant flux of 93.4 mW and dilution rate of 0.01 h⁻¹, *C. vulgaris* achieved a specific growth rate of 0.00925 h⁻¹. On decreasing the radiant flux alone from 119.2 mW to 93.4 mW while CO₂ concentration and dilution rate were constant at 5% (v/v) and 0.01 h⁻¹, the growth rate decreased by 62%. Similarly, increasing the CO₂ concentration alone from 5% (v/v) to 10% (v/v) while maintaining the radiant flux at 93.4 mW and dilution rate at 0.01 h⁻¹, a 42% decrease in growth rate was observed. However, a simultaneous increase in CO₂ concentration from 5% (v/v) to 10% (v/v) and radiant flux from 93.4 mW to 119.2 mW resulted in a 7% increase in growth rate. This demonstrates the importance of the combination effects of light intensity and CO₂ concentration to achieve high growth rates.
- It should be noted that this is the first time that the maximum specific growth rate for *C. vulgaris* has been studied, based on cell concentration, in a continuous stirred photobioreactor. Under the many environmental conditions studied in the continuous bioreactor, the growth rate of *C. vulgaris* did not exceed 0.01 h⁻¹. This value is approximately one order of magnitude smaller than the growth rate of yeast and bacteria growing aerobically on organic substrates. But considering that the *C. vulgaris* is a photoautotrophic organism that utilizes CO₂ and light energy for its growth, a lower growth rate compared to yeast is tolerable. Furthermore, by utilizing enhanced bioreactor design, such as the novel airlift photobioreactor in this study, it is likely that the growth rate of *C. vulgaris* could achieve a significantly higher value in a continuous flow bioreactor.

4.2. RECOMMENDATIONS

4.2.1. Novel Circulating Loop Photobioreactor

- An increase in light intensity has proven to increase the growth rate of *C. vulgaris*. Also, the best concentration for growth of *C. vulgaris* has been found to be 5% CO₂. A combination of the best CO₂ concentration at a higher light intensity and additional 8 hour dark phase could further enhance growth rates.
- The spectra of LED lights used had a lower irradiance in the red region of visible light. Studies by Powell *et al.* (2009a) showed that red light was highly effective in increasing specific growth rate of *C. vulgaris*. Hence, use of lights with higher irradiance in the red region of visible light in the circulating loop photobioreactor could further increase specific growth rate of *C. vulgaris*.
- The amount of CO₂ consumed in the bioreactor will help determine the photosynthetic efficiency of *C. vulgaris*. Also, this will provide an insight into the actual metabolic patterns of *C. vulgaris*. The success of an additional 8 hour dark phase has been proven in this study. However, a study of the difference in CO₂ consumption between no dark phase, short intervals of light-dark phase and a continuous 8 hour dark phase may provide valuable information required to optimize the growth rate of *C. vulgaris*.
- Higher concentrations of CO₂ (15% (v/v) and 10% (v/v)) was found to be stressful for growth of *C. vulgaris*. Hence, a study of lower concentrations of CO₂ in the range 0% (v/v) to 5% (v/v) will be beneficial to confirm the optimum concentration of CO₂ for growth of *C. vulgaris*.
- Interestingly, the biolipid concentration was also found to be affected by variation in light intensity and CO₂ concentration. An examination of the concentration of biolipids could be an interesting study to determine the commercial value of algal biomass produced in the complete microbiological fuel cell proposed by Powell *et al.* (2009b).

4.2.2. Continuous Flow Mixed Photobioreactor

- At higher dilution rates, the toxic effects of high concentration of CO₂ and high light were neutralized. Hence, higher growth rates of *C. vulgaris* maybe obtained by increasing the dilution rate greater than 0.01 h⁻¹ for CO₂ concentration of 15% (v/v) and radiant flux of 119.2 mW.
- Although high dilution rates are suitable for high concentrations of CO₂, at low concentrations of CO₂, high dilution rates have a distinct effect on growth rate. Hence, the effect of higher dilution rates on concentrations of CO₂ less than 10% (v/v) should be studied.
- An increase in growth rate was observed by decreasing dilution rates at low concentration of 5% (v/v) CO₂. A possible increase in growth rate may also be observed on decreasing the dilution rate at lower concentrations of CO₂.

5.0 REFERENCES

- Adir, N., Zer, H., Shochat, S., & Ohad, I. (2003). Photoinhibition- A Historical Perspective. *Photosynthesis research* , 343-370.
- APHA (American Public Health Association). (1999). Standard Methods for the Examination of Water and Wastewater (20th edition), Washington, D.C.
- Axelsson, L. & Beer, S. (2001). Carbon limitation. In: Rai, & J. P. Gaur (editors), *Algal adaptation to environmental stresses* (22-45). New York: Springer.
- Bailey, J. E., & Ollis, D. F. (1986). *Biochemical Engineering Fundamentals* (2nd edition). United States: McGraw Hill.
- Barsanti, L., & Gualtieri, P. (2006). *Algae-Anatomy, biochemistry and biotechnology*. Boca Raton: Taylor & Francis.
- Becker, W. (2004). Microalgae in human and animal nutrition. In: Richmond, A editor. *Handbook of microalgal culture: biotechnology and applied phycology*. Blackwell Publishing (312-346).
- Behrens, P. W. (2005). Photobioreactors and fermentors: the light and dark sides of growing algae. In *Algal Culturing Techniques* (189-199). Academic Press.
- Benemann, J. R. (2001). Wastewater treatment, greenhouse gas mitigation and hydrogen production using microalgae. In: K. Hiroyuki, & L. Yuan Kun (editors), *Photosynthetic microorganisms in environmental biotechnology* (2-9). Hong Kong: Springer.
- Berger, C. (Ed.). (1968). *Handbook of Fuel Cell Technology*. New Jersey: Prentice-Hall.
- Bond, D. R., & Lovley, D. R. (2003). Electricity Production by *Geobacter sulfurreducens* Attached. *Applied and Environmental Microbiology* , 1548-1555.

- Brown, J. W. (2009, April 3). MB451 *Microbial diversity*. Retrieved June 12, 2009, from NC State University, Department of Microbiology:
http://www.mbio.ncsu.edu/MB451/lab/plate_count/PCA.html
- Brown, L. M. (1996). Uptake of carbon dioxide from flue gas by microalgae. *Energy Conversion and Management* , 1363-1367.
- Chisti, M. Y. (1989). *Airlift Bioreactors*. London: Elsevier science publishers ltd.
- Chisti, M. Y., Camacho, G. F., Fernandez, A. F., & Grima, M. E. (1999). Photobioreactors: light regime, mass transfer and scaleup. *Journal of Biotechnology* , 231-247.
- Chisti, M. Y. (2007). Biodiesel from microalgae. *Biotechnology Advances* , 294-306.
- Clauwaert, P., Boon, N., Van der ha, D., Verhaege, M., Rabaey, K., & Verstraete, W. (2007a). Open Air Biocathode Enables Effective Electricity Generation with Microbial Fuel Cells. *Environmental science and technology* , 7564-7569.
- Clauwaert, P., Boon, N., Verstraete, W., Rabaey, K., Schampelaire, L. d., Pam, T. H., et al. (2007b). Biological Denitrification in Microbial Fuel Cells. *Environmental Science and technology* , 3354-3360.
- Cohen, B. (1931). The Bacterial Culture as an Electrical Half-Cell, *Journal of Bacteriology*, 21, 18-19
- Fogg, G. (2001). Algal adaptation to stress-some general remarks. In: Rai, & J. P. Gaur (editors), *Algal adaptation to environmental stresses* (1-17). New York: Springer.
- Fogg, G. E. (1954). *The metabolism of algae*. New York: John Wiley & sons, Inc.
- Geider, R. J., & Osborne, B. A. (1992). *Algal Photosynthesis - The measurement of algal gas exchange*. New York : Chapman and Hall.
- Goldman, J. C., Oswald, W. J., & Jenkins, D. (1974). The Kinetics of Inorganic Carbon Limited Algal Growth. *Water Pollution Control Federation* , 554-574.

- Govindjee & Whitmarsh, J. (1999). The photosynthetic process. In: G. S. Singhal, R. Renger, K.-D. Sopory, Irrang, & Govindjee (editors), *Concepts in photobiology: Photosynthesis and Photomorphogenesis* (11-47). New Delhi: Narosa Publishing House.
- Gregory, K. B., Bond, D. R., & Lovley, D. R. (2004). Graphite electrodes as electron donors for anaerobic respiration. *Environmental Microbiology* , 596-604.
- Hart, A. B., & Womack, G. J. (1967). *Fuel cells - Theory and application*. Netherlands: Nederlandse Boekdrukinrichting N. V
- Hill, G. A. (2006). Measurement of overall volumetric mass transfer coefficients for carbon dioxide in a well-mixed reactor using a pH probe. *Industrial and Engineering Chemistry Research* , 5796-5800.
- Hirata, S., Hayashitani, M., Taya, M., Tone, S. (1996). Carbon dioxide fixation in batch cultures of *Chlorella* sp. using a photobioreactor with a sunlight collection device. *Journal of Fermentation Bioengineering*. 470-472.
- Ieropoulos, I. A., Greenman, J., Melhuish, C., & Hart, J. (2005). Comparative study of three types of microbial fuel cell. *Enzyme and microbial technology* , 238-245.
- Javanmardian, M., & Palsson, B. O. (1991). High-density photoautotrophic algal cultures: design, construction and operation of a novel photobioreactor system. *Biotechnology and Bioengineering* , 1182-1189.
- Javanmardian, M., & Palsson, B. O. (1992). Continuous photoautotrophic cultures of the eukaryotic alga *Chlorella vulgaris* can exhibit stable oscillatory dynamics. *Biotechnology and Bioengineering* , 487-497.
- Kim, B. H., Chang, I. S., & Gadd, G. M. (2007). Challenges in microbial fuel cell development and operation. *Applied Microbiology and Biotechnology* , 485-494.
- Kleinheinz, G. T., & Keffer, J. E. (2002). Use of *Chlorella vulgaris* for carbon dioxide mitigation in a photobioreactor. *Journal of Industrial Microbiology and Biotechnology* , 275-280.

- Kordesch, K. V., & Simader, G. R. (1995). *Environmental impact of fuel cell technology*. Chemical Review, 95, Retrieved February 1, 2008, from <http://pubs.acs.org.cyber.usask.ca/>
- Lam, K. B., Chiao Mu & Lin Lewei (2003). A Micro Photosynthetic Electrochemical Cell. *IEEE*, 391-394.
- Lee, C.-G. and Palsson, B. O. (1995). Light-Emitting Diodebased algal photobioreactor with external gas exchange. *Journal of fermentation and bioengineering*, 257-263.
- Lee, C.-G. and Palsson, B. O. (1996). Photoacclimation of *Chlorella vulgaris* to Red Light from Light-Emitting Diodes Leads to Autospore Release Following Each Cellular Division, *Biotechnology progress*, 249-256
- Lee, J. M. (1992). Biochemical Engineering. New Jersey: Prentice Hall.
- Lee, Yuan-Kun & Shen, Hui. (2004). Basic Culturing Techniques. In: Richmond, A (editor). *Handbook of microalgal culture: biotechnology and applied phycology*. Cornwall: Blackwell Publishing (40-54).
- Logan, B. E., & Regan, J. (2006). Microbial Fuel Cells- Challenges and Applications. *Environmental Science and Technology* , 5172-5180.
- Matthijs, H. C. P., Balke, H., Van Hes, U. M., Kroon, B. M. A., Mur, L. R. & Binot, R. A. (1996), Application of Light- Emitting Diodes in Bioreactors: Flashing Light Effects and Energy Economy in Algal Culture (*Chlorella pyrenoidosa*). *Biotechnology and Bioengineering*, 98-107.
- Masojidek, J., Koblizek, M., & Torzillo, G. (2004). Photosynthesis in Microalgae. In: Richmond, A editor. *Handbook of microalgal culture: biotechnology and applied phycology* , 20-39.
- McDougall, A. (1976). *Fuel cells*. Great Britain: John Wiley & Sons, Inc.
- Merchuk, J. C., Siegel, M. C. (1988). Mass transfer in a rectangular airlift reactor: effects of geometry and gas recirculation. *Biotechnology and Bioengineering*, 1128-1137.

- Merchuk, J. C., Gluz, M., & Mukmenev, I. (2000). Comparison of photobioreactors for cultivation of the red microalga *Porphyridium* sp. *Journal of Chemical Technology and Biotechnology*, 1119-1126.
- Morita, M., Watanabe, Y. & Saiki, H. (2000). Investigation of photobioreactor design for enhancing the photosynthetic productivity of microalgae. *Biotechnology and Bioengineering*, 693-698.
- Mohan, Y., Muthu Kumar, S. M., & Das, D. (2008). Electricity generation using microbial fuel cells. *International Journal of Hydrogen Energy*, 423-426.
- Muranaka, T. & Murakami, M. (2001). CO₂ fixation by a high temperature high CO₂ tolerant *Chlorella* sp. In: Lee, Yuan-Kun, Hiroyuki, K. (editors). *Photosynthetic microorganisms in environmental biotechnology*, 77-86.
- Myers, J. and Killam, A. (1956). A Special Effect of Light on the Growth of *Chlorella vulgaris*. *American Journal of Botany*, 569-572.
- Najafpour, G. D. (2007). *Biochemical Engineering and Biotechnology*. Elsevier.
- Nielsen, J., Villadsen, J., & Liden, G. (2003). *Bioreaction Engineering Principles*. New York: Plenum Press.
- Nikakhtari, H., & Hill, G. A. (2005). Enhanced oxygen mass transfer in an external loop airlift bioreactor using packed bed. *Industrial and Engineering Chemistry Research*, 1067-1072.
- Noll, K. (2006). Microbial fuel cells. In N. Sammes, *Fuel Cell Technology: Reaching Towards Commercialization. Engineering Materials and Processes*, 278-296.
- Okpokwasili, G. C., & Nweke, C. O. (2005). Microbial growth and substrate utilization kinetics. *African journal of biotechnology*, 305-317.
- Packer, M. (2009. In press). Algal capture of carbondioxide : biomass generation as a tool for greenhouse gas mitigation with reference to New Zealand energy strategy and policy. *Energy policy* .doi:10.1016/j.enpol.2008.12.025

- Prasad, D., Sivaram, T. K., Berchmans, S., & Yegnaraman, V. (2006). Microbial fuel cell constructed with a micro-organism isolated from sugar industry effluent. *Journal of Power sources* , 991-996.
- Perner-Nochta, I., & Posten, C. (2007). Simulations of light intensity variation in photobioreactors. *Journal of Biotechnology* , 276-285.
- Powell, E. E., Mapiour, M. L., Evitts, R. W., & Hill, G. A. (2009a). Growth kinetics of *Chlorella vulgaris* and its use as a cathodic half cell. *Biosource Technology* , 269-274.
- Powell, E. E., Bolster, J, Evitts, R. W., & Hill, G. A. (2009b). An entirely microbiological fuel cell: A photosynthetic microalgae cathodic half cell coupled to a yeast anodic half cell. *Biochemical Engineering Journal*. Submitted.
- Porra, R. J. (2006). Spectrometric Assays for Plant, Algal and Bacterial Chlorophylls. In: B. Grimm, R. J. Porra, W. Rüdiger, & H. Scheer (eds.), *Chlorophylls and Bacteriochlorophylls: Biochemistry, Biophysics, Functions and Applications* (95-107). Netherlands: Springer.
- Rosenbaum, M., Schroder, U., & Scholz, F. (2005). Utilizing the green alga *Chlamydomonas reinhardtii* for microbial electricity generation: a living solar cell . *Applied Microbiology and Biotechnology* , 753-756.
- Siegel, M. H., & Merchuk, J. C. (1988). Airlift reactors in Chemical and Biological Technology. *Journal of Chemical Technology and Biotechnology* , 105-120.
- Siegel, M. H., Merchuk, J. C., & Schugerl, K. (1986). Airlift reactor analysis: Interrelationships between riser, downcomer, and gas-liquid separator behaviour including gas recirculation effects. *AIChE Journal* , 1585-1596.
- Shukla, A. K., Suresh, P., Berchmans, S., & Rajendran, A. (2004). Biological Fuel Cells and their application. *Current Science*, 87, 455-468.
- Shuler, M. L., & Kargi, F. (2002). *Bioprocess Engineering*. New Jersey: Prentice Hall.
- Suh, I. S., & Lee, S. B. (2001). Cultivation of cyanobacterium in an internally radiating air-lift photobioreactor. *Journal of applied phycology* , 381-388.

- Tokusoglu, O., & Unal, M. K. (2003). Biomass nutrient profiles of three microalgae: *Spirulina platensis*, *Chlorella vulgaris*, and *Isochrysis galbana*. *Journal of food science* , 1144-1148.
- Velásquez-Orta, S. B., Curtis, T. P. and Logan, B. E. (2009). Energy from algae using microbial fuel cells. *Biotechnology and Bioengineering*, 1068-1076.
- Yanagi, M., Watanabe, Y., & Saiki, H. (1995). Carbon dioxide fixation by *Chlorella* sp HA-1 and its utilisation. *Energy Conversion and Management* , 713-716.
- Young, A. J., Tsavalos, A. J., & Harker, M. (1996). Autotrophic growth and carotenoid production of *Haematococcus pluvalis* in a 30 liter air-lift photobioreactor. *Journal of fermentation and bioengineering* , 113-118.

APPENDIX A

Calculation of Light Intensity Incident on Continuous Flow Mixed Photobioreactor

Table A.1 Readings obtained from Spectrophotometer when light source was placed at 10 centimeters from surface of bioreactor and when no light source (reference) was used.

Wavelength	Dark	Counts
403.7	209	281
404.06	209	399
404.42	209	458
404.78	205	377
405.15	211	314
405.51	213	292
405.87	210	282
406.23	208	289
406.59	212	295
406.95	212	306
407.31	213	282
407.67	209	255
408.03	211	230
408.39	209	220
408.75	210	222
409.11	211	215
409.47	208	215
409.83	209	215
410.19	211	213

Sample Calculation of Radiant Flux Density for the Continuous Flow Mixed Photobioreactor

Consider the readings obtained at 403.7 nm:

Difference in counts between reference and reading for light source = $281 - 209 = 72$

$$\begin{aligned}
\text{Intensity of light at 403.7 nm} &= (1.65406 \times 10^{-14} \times 403.7^5) - (4.67109 \times 10^{-11} \times 403.7^4) + \\
&\quad (5.22642 \times 10^{-8} \times 403.7^3) - (2.88172 \times 10^{-5} \times 403.7^2) + \\
&\quad (7.79064 \times 10^{-3} \times 403.7) - (8.19587 \times 10^{-1}) \\
&= 0.31209 \mu\text{W}/\text{cm}^2\text{-nm}
\end{aligned}$$

Since, light intensity of light source used was too high for the spectrophotometer, frosted glass was used to attenuate the reading. The frosted glass was found to attenuate the reading by 86.06%

Therefore,

$$\begin{aligned}
\text{Corrected intensity at 403.7 nm} &= 0.31209 / (1-0.8606) \\
&= 2.2387 \mu\text{W}/\text{cm}^2\text{-nm}
\end{aligned}$$

Integral under the curve of Intensity versus Wavelength

$$\begin{aligned}
&= ((\text{Intensity at 403.7 nm} + \text{Intensity calculated for previous reading}) * (\text{Difference between wavelengths})) / 2 \\
&= ((2.2387 + 0) \times (403.7 - 403.34)) / 2 \\
&= 0.40298 \mu\text{W}/\text{cm}^2
\end{aligned}$$

$$\text{Accumulated energy until 403.7 nm} = 0.40298 \mu\text{W}/\text{cm}^2$$

Now, to calculate the Radiant Flux Density for the reactor, the accumulated energy for the whole spectrum of the light source is determined.

$$\text{Accumulated Energy} = 710.3475 \mu\text{W}/\text{cm}^2$$

Radiant Flux Density, at high intensity, for the Continuous Flow Mixed Photobioreactor

$$\begin{aligned}
&= (\text{Corrected Intensity}) * (\text{Surface area on which light shines}) / \\
&\quad (\text{Complete surface area of reactor})
\end{aligned}$$

$$\begin{aligned}
&= (710.3475 \times 167.84) / 939.366 \mu\text{W}/\text{cm}^2 \\
&= 0.1269 \text{ mW}/\text{cm}^2
\end{aligned}$$

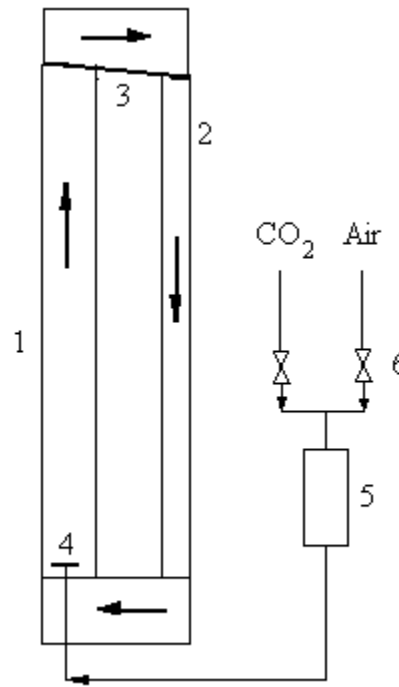
Radiant Flux Density, at low intensity, for the Continuous Flow Mixed Photobioreactor

$$\begin{aligned}
&= (556.569 \times 167.84) / 939.366 \mu\text{W}/\text{cm}^2 \\
&= 0.0994 \text{ mW}/\text{cm}^2
\end{aligned}$$

APPENDIX B

Calculation of Circulation Velocity in Circulating Loop Photobioreactor

Circulation length = length of riser + length of downcomer + diameter of riser + diameter of downcomer + (2 × distance between riser and downcomer)



- 1- Riser Section
- 2- Downcomer Section
- 3- Separation between riser and downcomer
- 4- Gas Sparger
- 5- Flow meter
- 6- Adjusting valve

Figure B.1 Schematic diagram of the photobioreactor.

$$\begin{aligned}
 \text{Therefore, circulation length} &= 47.44 + 47.44 + 2 + 1.5 + (2 \times 2) \text{ inches} \\
 &= 102.4 \text{ inches}
 \end{aligned}$$

$$= 3.058 \text{ meters}$$

The average circulation time was calculated using a trace dye at various heights of liquid in the reactor. Table B.1 shows the values obtained.

Table B.1 Data table showing calculated values of average circulation velocity for the circulating loop photobioreactor at varying heights of liquid in the reactor.

Height of liquid in reactor (m)	Average Circulation Time (seconds)	Velocity (m/s)
1.155	39.76	0.08
1.160	35.08	0.09
1.170	25.10	0.12
1.179	23.03	0.13
1.185	22.94	0.13
1.190	22.76	0.13
1.200	21.88	0.14
1.205	21.61	0.14

Circulation velocity obtained when the height of the liquid was maximum

$$= 1.205 / 21.61 \text{ m/s}$$

$$= 0.14 \text{ m/s}$$

Average circulation velocity for the reactor

$$= (0.08 + 0.09 + 0.12 + 0.13 + 0.13 + 0.13 + 0.14 + 0.14) / 8$$

$$= 0.12 \text{ m/s}$$

APPENDIX C

Calculation of Biolipid concentration of *C. vulgaris* by Soxhlet Extraction Method

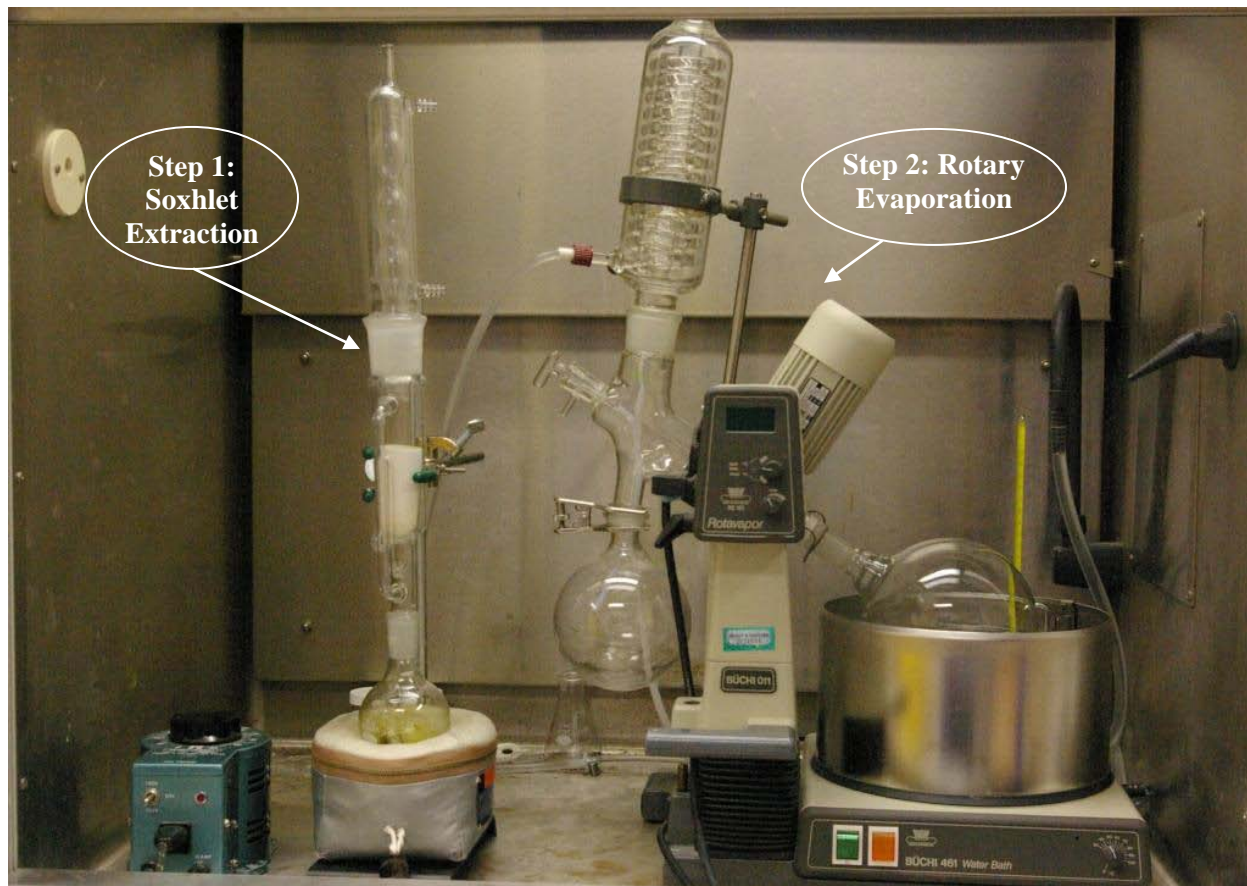


Figure C.1 Experimental set-up used for Soxhlet extraction.

Sample Calculation of algal lipids for sample obtained from circulating loop fed- batch reactor

Conditions in bioreactor when algal sample was obtained:

CO ₂ flowrate	15% (v/v); 30 ml/min
Air flowrate	85% (v/v); 170 ml/min
Light intensity	269.45 mW
Dry cell weight of sample	1.3914 g

Initial mass of thimble = 3.5399 g

Initial mass of thimble with algal sample	$= (3.5399 + 1.3914) \text{ g}$
	$= 4.9313 \text{ g}$
Initial mass of boiling flask with boiling chips	$= 108.3672 \text{ g}$
Final mass of thimble after evaporation	$= 4.7922 \text{ g}$
Final mass of boiling flask	$= 108.5806 \text{ g}$
Change in mass of thimble	$= (4.9313 - 4.7922) \text{ g}$
	$= 0.1391 \text{ g}$
Change in mass of boiling flask	$= (108.5806 - 108.3672) \text{ g}$
	$= 0.2134 \text{ g}$
% Lipids in algae sample	$= 0.1391 \text{ g} / 1.3914 \text{ g}$
(based on change in mass of thimble)	$= 0.09997$
	$= 10\%$